Surface and middle layer enrichment of dissolved copper in the western subarctic North Pacific

Iwao Tanita[1], Shigenobu Takeda[1), 2)], Mitsuhide Sato[1)]* and Ken Furuya[1)]

Abstract: Vertical distributions of dissolved copper were investigated at two stations in the western subarctic and tropical North Pacific to elucidate the factors controlling its concentration. There was a significant correlation (p-value <0.05) at the subarctic and tropical stations between dissolved copper and silicic acid between 400–3000 m and 300–2000 m depths, respectively, which implies the importance of diatoms in transporting copper. The dissolved copper concentration at depths shallower than 1000 m was 1.3–2.7 times higher at the subarctic station than that at the tropical station, and at depths shallower than 1500 m, it was 0.97–2.60 nM higher at the subarctic station than the average of other reported values of the North Pacific. This can be attributed to several processes. In the surface layer, horizontal advection of the coastal water by the East Kamchatka Current was considered to be a source of copper because a high concentration was observed within low-salinity surface waters. Supply of copper below the surface layer to 1500 m was probably owing to downward transport by the biological pump and horizontal advection. These results suggest that horizontal transport of copper from coastal or shelf area is important for biological production and Cu distribution in this region.

Keywords : *dissolved copper, North Pacific, subarctic, tropical*

1. Introduction

Copper (Cu) is a trace metal that is both a nutrient and toxin to phytoplankton. Copper is

1) Department of Aquatic Bioscience, Graduate School of Agricultural and Life Sciences, The University of Tokyo, 1-1-1 Yayoi, Bunkyo-ku, Tokyo, 113-8657, Japan
2) Department of Marine Science, Graduate School of Fisheries Science and Environmental Studies, Nagasaki University, Bunkyo-machi, 1-14, Nagasaki, 852-8521, Japan
 * Corresponding author:
 Tel: +813-5841-5292
 Fax: +813-5841-5308
 E-mail: asatom@mail.ecc.u-tokyo.ac.jp

required by phytoplankton, and works at the active center of a variety of Cu-containing proteins, such as plastocyanin, cytochrome oxidase, ascorbate oxidase, superoxide dismutase, and multicopper ferroxidase (Twining and Baines, 2013). It has often been pointed out that its concentration is low enough to limit phytoplankton growth (e.g., Moffett and Dupont, 2007). On the contrary, a surplus of Cu is toxic to phytoplankton (Coale, 1991). Cu toxicity may control the composition and growth of the natural phytoplankton community (Moffett et al., 1997; Mann et al., 2002; Paytan et al., 2009). These effects of Cu on phytoplankton are controlled by the spatiotemporal variability of its concentration

in the nanomolar range. Therefore, it is important to elucidate the spatial variability of Cu concentration to understand whether Cu supports or limits phytoplankton growth in the environment.

To understand the spatial variability of Cu, knowledge of its sources and sinks are important. Known sources of Cu are aerosol deposition (PAYTAN et al., 2009), riverine input (MARTIN and WHITFIELD, 1983), sediments in the coastal and shelf region (WESTERLUND and ÖHMAN, 1991), and hydrothermal vents (SANDER and KOSCHINSKY, 2011). Known sinks of Cu are consumption by organisms (KINUGASA et al., 2005) and scavenging with sinking particles (BOYLE et al., 1977; BRULAND, 1980). However, knowledge about spatial variation in Cu concentration in the open ocean has been limited to the subtropical Pacific and Atlantic Oceans (BOYLE et al., 1981; SAAGER et al., 1997).

To elucidate local sources and sinks of Cu, it is necessary to investigate its vertical profile. The typical vertical profile of dissolved Cu (D-Cu), which has been known since the late 1970's, is a hybrid-type of nutrient-type and scavenged-type. Since D-Cu has nutrient-type characteristics, its concentration is as low as 0.24 nmol l^{-1} in the surface water (BRULAND, 1980; MILLER and BRULAND, 1994; EZOE et al., 2004), owing to consumption by microorganisms, and increases in the middle to deep layer (BOYLE et al., 1977), owing to recycling associated with organic matter decomposition. Moreover, supply from bottom sediments and scavenging by particles throughout the column also affect the Cu profile (BOYLE et al., 1977). In addition, Cu supply by aerosol deposition (PAYTAN et al., 2009) in the surface or by horizontal advection in the surface and middle layer (YEATS and CAMPBELL, 1983) has also been reported.

The western North Pacific is a region with high Fe supply and its sources are aerosol deposition from the East Asia (MOORE and BRAUCHER, 2008) and horizontal transport from the Sea of Okhotsk into the intermediate water of the Western Subarctic Gyre (NISHIOKA et al., 2007). Although these processes can simultaneously supply Cu and Fe, the spatial variability of Cu concentration in this region is limited (FUJISHIMA et al., 2001; EZOE et al., 2004; TAKANO et al., 2014). The fact that Cu can be used as an alternative to Fe under Fe deficient conditions in some diatoms (PEERS and PRICE, 2006) implies that Cu is an important element for the phytoplankton in this Fe-limited high-nitrate low-chlorophyll (HNLC) region.

In this study, we report differences in the D-Cu concentration between the subarctic and tropical regions in the western North Pacific, and discuss the possible sources and sinks of D-Cu.

2. Materials and Methods
Sampling

Sampling was conducted during the KH-08-2 cruise of the R/V Hakuho-maru at subarctic Stn. 5 (47° 00′ N, 160° 07′ E, 5248 m depth, August 2008) and tropical Stn. 22 (11° 30′ N, 155° 00′ E, 5795 m depth, September 2008) in the western North Pacific (Fig. 1). Seawater was collected using acid-washed Teflon-coated Niskin-X bottles at depths from 5000 m to 5 m. Seawater for D-Cu samples was filtered through an acid-washed 0.22 -μm pore-sized Millipak 100 filter (Merck-Millipore) attached to a Teflon spigot of a Niskin-X bottle. Acid-cleaned 125 ml low-density polyethylene (LDPE) bottles (Nalgene) were used for D-Cu sampling. Before sampling, the bottles were cleaned as described in KONDO et al. (2012). After sampling, the D-Cu samples were acidified to a pH of 1.7 by adding hydrochloric acid (Tamapure-AA 100, Tama Chemicals).

Hydrography, chlorophyll *a* and nutrients

Vertical profiles of temperature, salinity, dissolved oxygen (DO), and fluorescence were
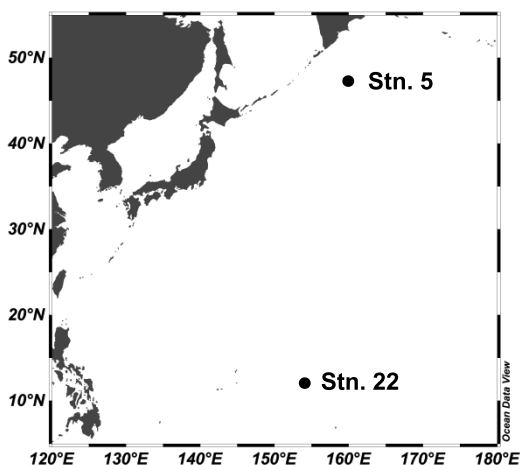
Fig. 1 Sampling was conducted at Stns. 5 (47° 00′ N, 160° 07′ E) and 22 (11° 30′ N, 155° 00′ E) during the KH-08-2 cruise of R/V Hakuho-maru (August-September 2008). The map was drawn using Ocean Data View (SCHLITZER, 2012).

monitored by sensors (Sea-bird Electronics) attached to a rosette. The mixed layer depth was defined to be where there was a 0.125 increase in sigma-t compared to that at the 10 m depth (SUGA et al., 2004). The Brunt-Väisäla frequency was calculated from vertical profiles of temperature and salinity as described by MILLARD et al. (1990). Apparent oxygen utilization was calculated by subtraction of the ambient DO concentration from the DO saturated concentration (WEISS, 1970). 113–300 ml of seawater for chlorophyll a (Chl. a) analysis was filtered through 25-mm glass microfiber filters (GF/F, Whatman), and the Chl. a concentrations were measured fluorometrically using a 10-AU fluorometer (Turner Designs) after extraction with 5 ml of N', N'-dimethylformamide on board. Seawater for nutrient analysis was frozen at −20 ℃. Concentrations of nutrients were measured by an autoanalyzer (AACS III, Bran + Luebbe) on land. The salinity of the surface water pumped up from the bottom of the ship (5 m) was also monitored

(ACT-20, Alec Electronics) during the cruise. The surface sensor was calibrated against discretely determined salinity of seawater collected from the sea surface by bucket sampling during the leg 1 of this cruise (stations not shown).

Reagents for dissolved copper

Salicylaldoxime (SA) (Sigma) was dissolved in 0.1 mol l^{-1} hydrochloric acid (Tamapure-AA 100, Tama Chemicals) at a concentration of 10 mmol l^{-1}, to be used as a stock solution, and left at 4–6 ℃ for a few days to achieve complete dissolution. For the second measurements without UV irradiation described later, SA was dissolved in Milli-Q water at 100 mmol l^{-1} and was used as a stock solution. It was heated in a microwave oven for complete dissolution before use. Then, it was diluted with Milli-Q water to a final concentration of 10 mmol l^{-1} and used as the working solution. Boric acid (suprapure, Merck-Millipore) was dissolved in 0.35 mol l^{-1} ammonia water (Tamapure-AA 100, Tama Chemicals) at a final concentration of 1 mol l^{-1} to obtain the pH buffer. For additional measurements, the borate buffer was purified twice by the MnO_2 method (GRASSHOFF et al., 1999). 3-[4-(2-Hydroxyethyl)-1-piperazinyl]-propanesulfonic acid (EPPS) (Sigma-Aldrich) was dissolved in 1 mol l^{-1} ammonia water (Tamapure-AA 100, Tama Chemicals) at a final concentration of 1.2 mol l^{-1} to be used as another pH buffer. A standard Cu solution was prepared by serial dilution from copper standard solution (Cu: 1,000 mg l^{-1}, JCSS, $Cu(NO_3)_2$ in 0.1 mol l^{-1} HNO_3, Wako Pure Chemical Industries) with 0.05-0.1 mol l^{-1} hydrochloric acid (Tamapure-AA 100, Tama Pure Chemical Industries).

Measurement of dissolved copper

D-Cu concentration was measured by cathodic stripping voltammetry (CSV) using SA (CAMPOS and VAN DEN BERG, 1994). Measurement of D-Cu

concentration was conducted after 16 months of preservation. Twelve milliliters of samples were pipetted in a quartz tube and UV-irradiated for 4 hours (CAMPOS and VAN DEN BERG, 1994) at 80–90 ℃ by a 705 UV digester with a 150 W lamp (Metrohm) to decompose dissolved organics that could interfere with the CSV measurement by preventing Cu from forming a complexation with SA or saturate at the surface of the mercury drop of the working electrode. After irradiation, 10 ml of the sample was neutralized to a pH of 8.3–8.4 with 100 μl of borate buffer and ammonia water (Tamapure-AA 100, Tama Chemicals). SA was added at a final concentration of 25 μmol $^{-1}$. Then the Teflon$^{®}$ perfluoroalkoxy (PFA) measuring vessel (Metrohm) was set at 757 or 797 VA Computrace (Metrohm). The voltammetric setting was slightly modified from that of CAMPOS and VAN DEN BERG (1994). Deposition potential was set at −1.06 V. The scan range was from −0.11 to −0.56 V. The concentration of D-Cu was determined using the standard addition method. The detection limit was 0.05 nmol l^{-1}, which is three times the standard deviation of the peak height obtained by the replicate measurement of Cu in Milli-Q water. The measured concentration of standard seawater (NASS-5), using the EPPS buffer (final concentration of 6.0 mmol l^{-1} and final pH of 8.3=8.4) without UV irradiation, was 5.16 ± 0.19 nmol l^{-1} (n = 3), which is within the range of the certified values of 4.67 ± 0.72 nmol l^{-1}. Although we used the EPPS buffer in the beginning, it was later replaced by the borate buffer to eliminate the effect of the EPPS complexing with copper (SOARES and BARROS, 2001). Moreover, since the conditional stability constant of Cu-EPPS is much weaker than that of Cu-SA, the effect of EPPS on the measurements was negligible. Therefore, data measured using each buffer was treated equally in this study.

In the first measurement, we conducted UV irradiation on the sample seawater. However, we left out this process in the second measurement, because measurements of SAFe reference samples S and D2 without UV irradiation (n =3; 0.50 ± 0.03 and 2.35 ± 0.15 nmol l^{-1} for S and D2, respectively) agreed with consensus values of 0.52 ± 0.05 and 2.28 ± 0.15 nmol kg^{-1} for S and D2, respectively, reported in May 2013 (www. geotraces.org). The voltammetric setting was the same as described by CAMPOS and VAN DEN BERG (1994). Values determined without UV irradiation were at 3500 and 4500 m at Stn. 5 and at 5 and 50 m at Stn. 22, which are realistic values compared with values just above and below the depth measured with UV irradiation. Some values were the average of results by both methods with and without UV irradiation at 5, 50, 150, and 1500 m at Stn. 5 and at 10 m at Stn. 22 because no clear difference was observed between the results with and without UV irradiation (data not shown).

Blanks were corrected assuming that the Cu concentration in Milli-Q water was zero. Since the pH buffer varied between measurements, we measured blanks separately for these different measurements (the final pH was the same in both measurements). Thus, the reported values in this study are comparable to each other despite the different pH buffers used.

Phytoplankton Pigment Composition

To analyze phytoplankton pigment composition, 0.7–5.2 l of seawater collected from 5, 10, 20, 30, and 50 m at Stn. 5 and from 5, 10, 30, 50, 100, 140, 150, and 200 m at Stn. 22 was filtered through glass microfiber filters (GF/F, Whatman). The filters were flash-frozen in liquid nitrogen or frozen at −80 ℃ in a freezer, and were preserved at −80 ℃ until analysis on land. Pigments on the filters were extracted in 3.6 ml of 95% methanol (for liquid chromatography, Wako Pure Chemical Industries) with sonification (Sonifier 150,

Branson) to destroy phytoplankton cells. After > 1 h extraction at 5 ℃, glass microfiber filters in the extracts were eliminated by filtration using a 0.2-μm polytetrafluoroethylene (PTFE) syringe driven filter unit (Millex®-FG, Merck-Millipore). Finally, 1.6 ml of the extract was mixed with 0.4 ml of Milli-Q water just prior to injection into a high-performance liquid chromatography (HPLC) system.

Pigments in the extracts were quantified by HPLC according to a method of ZAPATA et al. (2000) slightly modified as MIKI et al. (2008). The measured pigments were identified by comparing retention time and absorbance spectra with those of standard pigments. Data of absorbance and spectra used in this study were from FURUYA et al. (2003) and MIKI et al. (2008). The measured pigments were monovinyl (MV) Chl. a, MV Chl. b, divinyl (DV) Chl. a, zeaxanthin (Zea), alloxanthin (Allo), diadinoxanthin (Diad), 19´-hexanoyloxyfucoxanthin (Hex), prasinoxanthin (Pras), fucoxanthin (Fuco), 19´-butanoyloxyfucoxanthin (But), peridinin (Peri), Chl. c_3, Neoxanthin (Neo), and Chlorophyllide a (Chld. a).

3. Results

Hydrography, chlorophyll a, phytoplankton pigments and nutrients

Salinity monotonically increased with depth at Stn. 5 from 32.6 at the surface to 34.7 at 5000 m depth (Fig. 2a). Potential temperature at Stn. 5 was highest (13.2 ℃) at the surface, sharply decreased with depth, and was minimum (1.14 ℃) at 93 m. Then, temperature increased to about 3.67 ℃ at 256 m, and decreased again with depth to 1.08 ℃ at 5009 m (Fig. 2a). At Stn. 22, salinity was stable at 34.6 at the surface (at 43 m), and increased with depth to its maximum (35.1) at 158 m (Fig. 2b). The salinity maximum is typical of North Pacific Tropical Water (SUGA et al., 2000). Salinity, then decreased and reached a
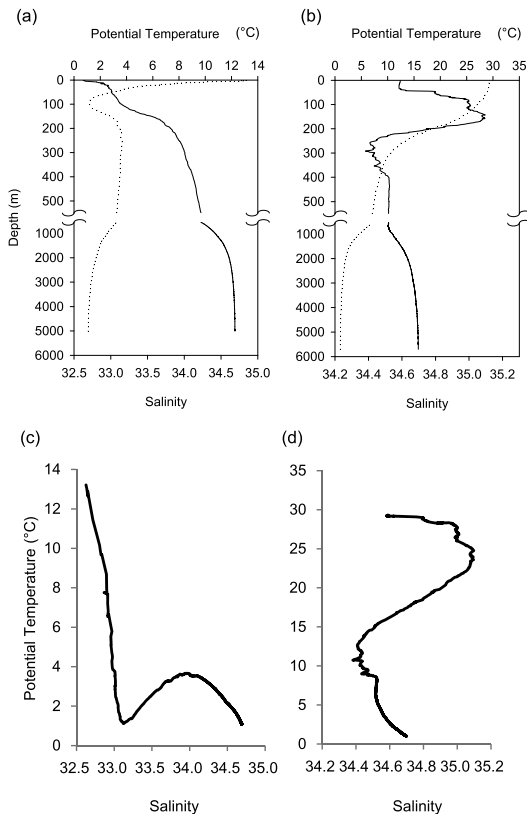

Fig. 2 Salinity (solid line) and Potential temperature (dotted line) profiles at Stns. 5 (a) and 22 (b). T-S diagrams were also depicted from these data at Stns. 5 (c) and 22 (d).

minimum (34.4) at 292 m, and increased again with depth to 34.7 at 5702 m. Potential temperature at Stn. 22 was the highest (29.3 ℃) at the surface and monotonically decreased to 1.01 ℃ at 5702 m (Fig. 2b).

The hydrography at Stn. 5 was categorized into two water masses, Subarctic Upper Water (0–2000 m) and Pacific Deep Water (2000–5000 m) (Fig. 2c), based on temperature and salinity (TOMCZAK and GODFREY, 2005). At Stn. 22, the Western North Pacific Central Water, North Pacific Intermediate Water, and Pacific Deep Water (TOMCZAK and GODFREY, 2005) were observed at depths of approximately 175–250 m,

250–2000 m and 2000–5702 m, respectively (Fig. 2d). Water masses with low salinity at depths shallower than 175 m were not denominated as far as we know, but probably resulted from the formation of high-salinity North Pacific Tropical Water (Suga *et al.*, 2000) observed around 175 m. That is, high-salinity water mass was formed around the sea surface by evaporation and was subsided owing to its high density while being transported laterally, which resulted in more saline subsurface water than the surface one. The mixed layer depth (MLD) was 12 m and 45 m at Stns. 5 and 22, respectively. At Stn. 5, the Brunt-Väisälä frequency sharply increased around the bottom of the mixed layer from 0.0509 at 11 m to 0.204 at 12 m, and then decreased with depth to 0.0552 at 200 m (Fig. 3a). The surface water at depths shallower than 12 m at Stn. 5 was characterized by low salinity (32.6–32.9) and was distinguishable in the T–S diagram (Fig. 2c). The low-salinity water in the sea surface (5 m) was widely observed in the northern area during the cruise (Fig. 4). At Stn. 22, the Brunt-Väisälä frequency was relatively stable (0.01–0.03) from 10 m to 43 m. Then, it sharply increased to 0.0553 at 46 m, coinciding with the mixed layer depth.
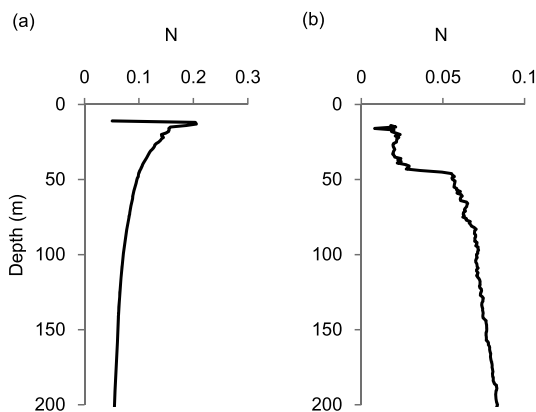
Below 46 m, it gradually increased with depth to 0.0834 at 200 m (Fig. 3b).

Chl. *a* concentration was highest at the surface (0.67 μg l^{-1}), and sharply decreased from the 50 to 100 m depth at Stn. 5 (Fig. 5a). Although a low Chl. *a* value (0.23 μg l^{-1}) was observed at 40 m, it is uncertain whether it was actually low or was caused by a mishandling of samples in the measurement because there was no drastic
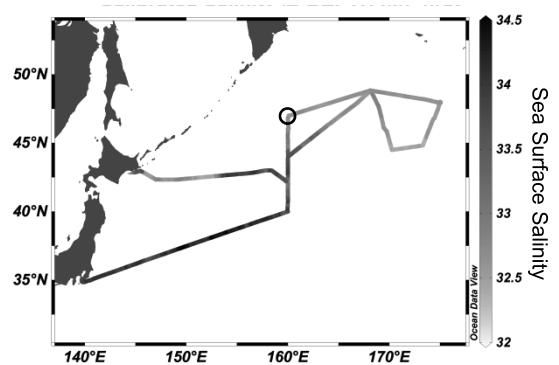

Fig. 4 Salinity on the surface during the first leg of the cruise (from 29 Jul to1 9 Aug 2008) was plotted on the map using Ocean Data View. Location of Stn. 5 was shown by a circle on the map.
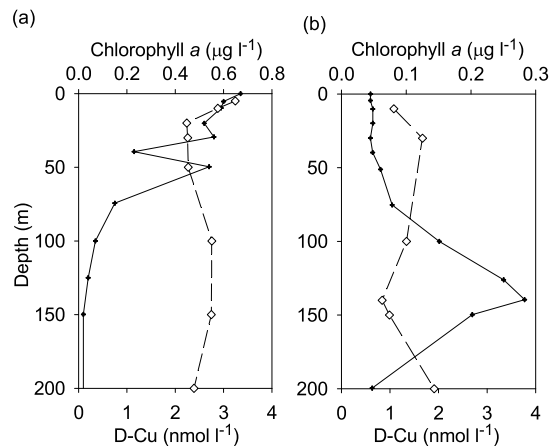

Fig. 3 Vertical distributions of Brunt-Väisälä frequency (N) were calculated from temperature and salinity at Stns. 5 (a) and 22 (b).

Fig. 5 Chlorophyll *a* (cross, solid line) and dissolved copper (white diamond, dashed line) at Stns. 5 (a) and 22 (b).

change of *in vivo* fluorescence, temperature, or salinity around this depth. At Stn. 22, Chl. *a* was low (0.04-0.08 μg l^{-1}) throughout the top 75 m and the subsurface Chl. *a* maximum was observed (SCM, 0.28 μg l^{-1}) at 140 m depth (Fig. 5b).

At Stn. 5, among the algal pigments determined in the present study, MV Chl. *a*, But, Hex, Fuco, Chl. *b*, Chl. c_3 and Diad were dominant (Table 1), implying that diatoms, prymnesiophytes and dinoflagellates were the dominant phytoplankton groups. At Stn. 22, the concentrations of MV and DV Chl. *a*, and Zea were high in the top 100 m. From SCM (140 m) to 150 m, Chl. *b* in addition to the above pigments was also abundant (Table 1). These results imply that the dominant phytoplankton groups were cyanobacteria and prochlorophytes. Although Fuco was also detected at Stn. 22, its concentration was low, which suggests a low abundance of diatoms.

The oxygen minimum was observed at 700 m (7.18 ml l^{-1}) and 1160 m (5.86 ml l^{-1}) at Stns. 5 and 22, respectively (Fig. 6a-d). The layers of the oxygen minima corresponded to the Subarctic Upper Water and the North Pacific Intermediate Water at Stns. 5 and 22, respectively.

Nitrate, phosphate, and silicic acid concentrations were lowest in the surface (7.52 μmol l^{-1}, 0.932 μmol l^{-1} and 8.76 μmol l^{-1}, respectively), and highest around 300-600 m for nitrate and phosphate (45.7-46.2 μmol l^{-1} and 3.17-3.19 μmol l^{-1}, respectively), and at 1500 m for silicic acid (163 μmol l^{-1}); all these values were observed to occur within the Subarctic Upper Water. At Stn. 22, nitrate, phosphate and silicic acid concentrations were lowest above the SCM, and had their maxima at 1000 m (40.3 μmol l^{-1}), 1500 m (2.90 μmol l^{-1}) and 3000 m (155 μmol l^{-1}), respectively. The concentration maxima occurred within the Western North Pacific Central Water and the North Pacific Intermediate Water for nitrogen and phosphorus and occurred deeper in the

Pacific Deep Water for silicon.

Dissolved copper

Vertical profiles of D-Cu had nutrient-type characteristics at both subarctic and tropical stations (Fig. 6b and d), although the relative variation in the D-Cu concentration between surface and deep waters was smaller than that in the nitrate concentration. At the subarctic Stn. 5, a relatively high concentration was observed near the surface (3.2 nmol l^{-1} at 5 m), within low-salinity water (32.6-32.9). Below the MLD (12 m), D-Cu concentration had its minimum (2.24-2.26 nmol l^{-1}) at 20-30 m, the region where Chl. *a* was still high (Fig. 5a). The range of D-Cu concentration was 2.2-3.2 nmol l^{-1} at a depth of 5-1000 m. The D-Cu concentration increased between 1000-1500 m and 3000-4000 m, and reached 5.0 nmol l^{-1} at a depth of 4000-5000 m (Fig. 6b). The D-Cu continued to increase below the layer of the AOU, nitrate, phosphate and silicic acid (Figs. 6a and b) maxima. The correlation between D-Cu concentration and silicic acid concentration (Fig. 7a) was significant between 400-3000 m ($p < 0.05$). On the other hand, no significant correlation was observed between D-Cu concentration and nitrate and phosphate concentration or AOU (not shown).

At the tropical Stn. 22, D-Cu concentration had its minimum (0.84 nmol l^{-1}) at SCM (140 m), although it was relatively constant within the surficial 200 m (Fig. 5b). We eliminated the D-Cu data at 5 m because heavy contamination was suspected (10.1 nmol l^{-1}). Increase of the D-Cu concentration was observed below 400 m depth in the North Pacific Intermediate Water, reaching 4.0-4.5 nmol l^{-1} at depths of 3000-5000m (Fig. 6d) in the Pacific Deep Water. Below this depth, the D-Cu further increased to 5.15 nmol l^{-1} at 5587 m, which was approximately 200 m above the sea floor. As observed at Stn. 5, the D-Cu continued increasing much below the AOU, nitrate, phos-
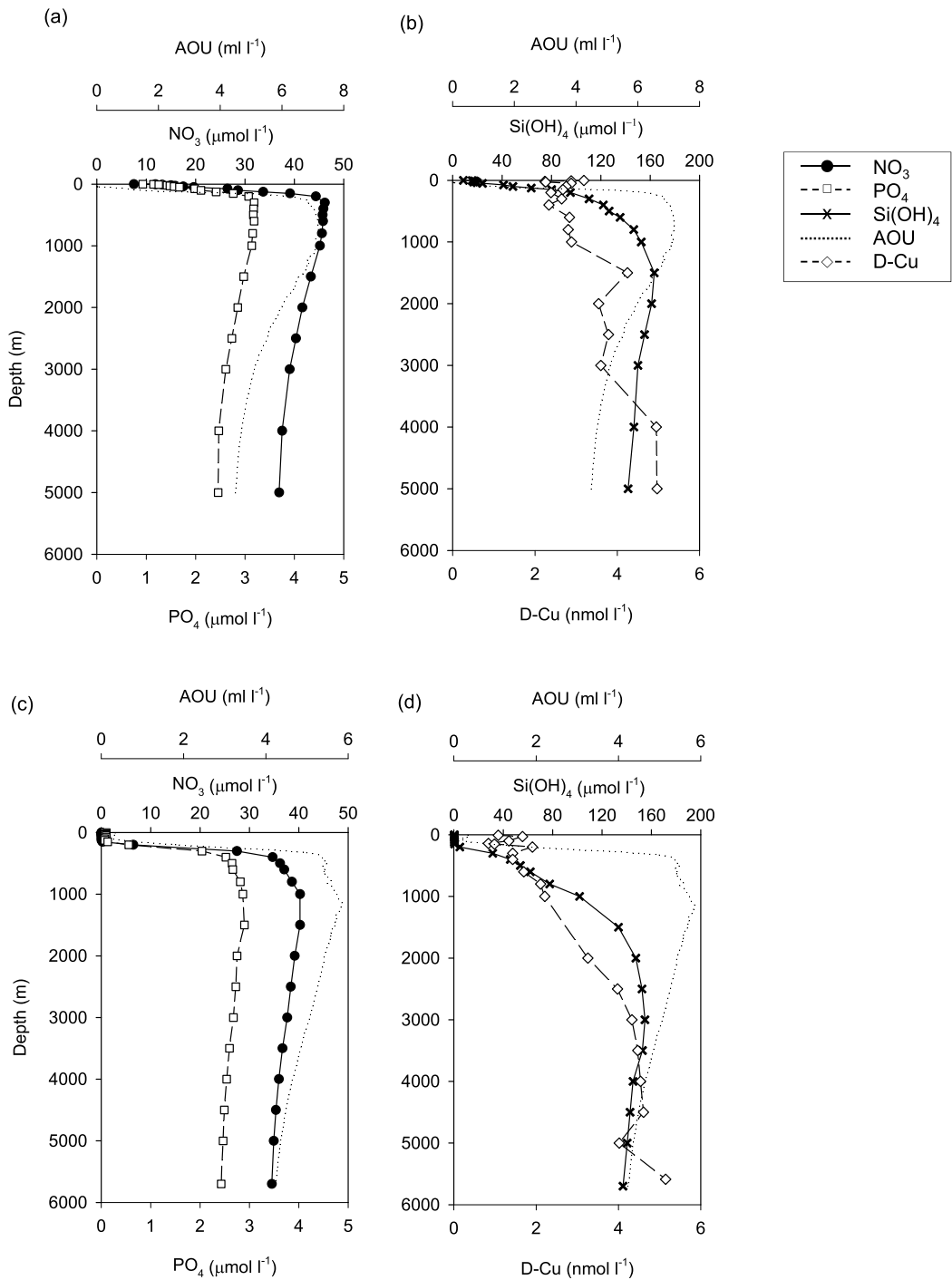
Fig. 6 Nitrate（a, c）, phosphate（a, c）, Silicate（b, d）, dissolved copper（b, d）and AOU（a, b, c, d）profiles at Stns. 5（a, b）and 22（c, d）.
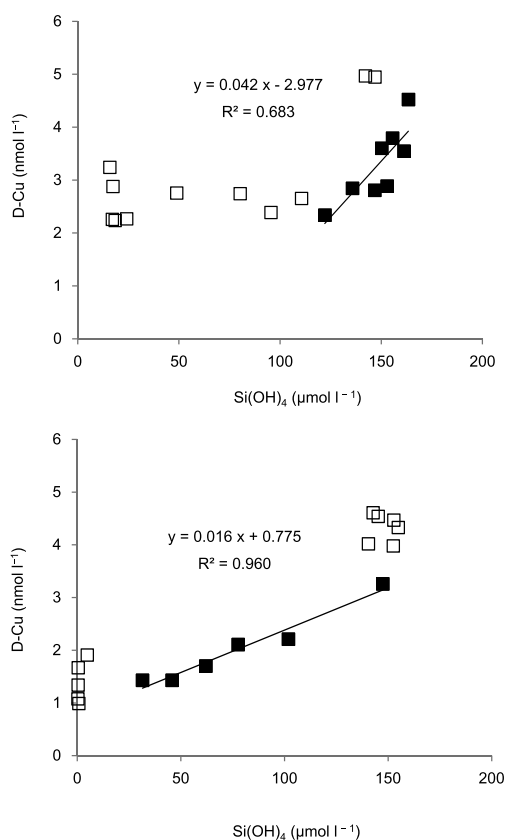
Fig. 7 Relationship between concentrations of dissolved copper and silicic acid at Stns. 5 (a) and 22 (b) throughout the water column (open and filled squares). Significant correlation was observed between 300–2000 m and 400–3000 m depth at Stns. 5 and 22, respectively (shown by filled squares, $p <0.05$).

phate, and silicic acid maxima at this station. Within a limited depth from 300–2000 m, the D-Cu concentration showed a significant correlation with the silicic acid concentration ($p <0.05$) (Fig. 7b). Below 2000 m, the silicic acid concentration was relatively constant, while the D-Cu continued to increase with depth, resulting in no significant correlation ($p >0.05$) within this depth range. The distribution of nitrate, phosphate, and AOU had no relationship with that of D-Cu ($p >0.05$).

With respect to Stns. 5 and 22, D-Cu was higher at Stn. 5 than at Stn. 22 at depths shallower than 1500 m, which corresponds to the Subarctic Upper Water at Stn. 5 and the Western North Pacific Central Water and the North Pacific Intermediate Water at Stn. 22. In contrast, the D-Cu was at the same level below 2000 m, which corresponds to the Pacific Deep Water at both stations.

4. Discussion
Characteristics of D-Cu profile

Nutrient-type characteristics of D-Cu profiles are commonly observed in the Atlantic (MOORE, 1978; YEATS and CAMPBELL, 1983; DANIELSSON *et al.*, 1985), the Pacific (BOYLE *et al.*, 1977; BRULAND, 1980), and the Indian Oceans (DANIELSSON, 1980; SAAGER *et al.*, 1992). The D-Cu concentration minimum coincided with the Chl. *a* concentration maximum at both subarctic and tropical stations, suggesting D-Cu consumption by phytoplankton. D-Cu concentration increased with depth below the middle depths (1000 and 600 m at Stns. 5 and 22, respectively), which is likely due to integrated effect of remineralization accompanied by organic matter decomposition and lateral transport of aged water mass by deep sea circulation (FEELY *et al.*, 2004).

In the present study, the correlation between D-Cu and silicic acid was observed at both Stns. 5 and 22, though in different depth ranges (Fig. 7). A correlation between D-Cu and silicic acid caused by Cu consumption by diatoms and the following downward transport through the biological pump has previously been reported (WESTERLUND and ÖHMAN, 1991; NOLTING *et al.*, 1991; LÖSCHER 1999; BOYE *et al.*, 2012). The slope of this correlation at Stn. 22 was 0.016 in this study, which is within the range of reported values in the subtropical and subarctic eastern North Pacific (0.006–0.029) (NOLTING *et al.*, 1991). In the

subtropical region, despite a generally low abundance of diatoms, a correlation between Cu and Si has previously been frequently observed (NOLTING *et al.*, 1991; BOYE *et al.*, 2012). In addition, at Stn. 22, which is located in the tropical region, the abundance of diatoms was low as shown by the low Fuco/Chl. *a* ratio (0.02–0.07) that is an order of magnitude lower than that at Stn. 5 (0.22–0.32). Moreover, the opal contribution to total sinking particle flux has also been reported to be lower in the western subtropical North Pacific than in the subarctic region (KAWAHATA, 2002). These observations imply that dissolved copper between 300 and 2000 m at Stn. 22 was mainly supplied by lateral transport from diatom-dominated high productive areas. In contrast, at Stn. 5, the correlation between Cu and silicic acid was not observed around the silicocline between 5–300 m. However, then, D-Cu increased below 400 m, where increase of silicic acid was small. This resulted in the larger slope (0.042) of the correlation at Stn. 5 (Fig. 7a) than that at Stn. 22 (0.016, Fig. 7b). To explain the fact that D-Cu kept increasing below the silicic acid maximum at both stations, it is necessary to consider downward transport of Cu by sinking particles other than diatoms, such as mineral particles, or supply of Cu from the bottom sediments (BOYLE *et al.*, 1977; BRULAND, 1980) even if Cu supply by lateral transport is taken into account. Since D-Cu gradient was observed from the bottom to 2000 m at Stn. 22 despite the low value at 5000 m, D-Cu increase between 2000–5587 m seems to have been attributed to the bottom source. On the other hand, discontinuity of D-Cu gradient was observed between 3000 m and 4000 m at Stn. 5. Therefore, supply from the bottom source at this station seems to have been limited between 4000 and 5000 m if lateral transport of water mass was not considered. Between 2000 and 3000 m, D-Cu may have been supplied by sinking mineral particles. Although mineral particles can also supply silicic acid together with Cu, its relative influence on silicic acid concentration seems to be low because the concentration of autochthonous silicic acid is high. On the contrary, D-Cu concentration can be relatively strongly influenced by supply from mineral particles because D-Cu concentration is initially low. In addition to the supply from mineral particles, supply by northern horizontal transport of Cu-rich water by deep-sea circulation is another possible reason to explain the discontinuity of D-Cu gradient. Therefore, it is necessary in the future study to elucidate vertical distributions of Cu from the high-resolution latitudinal survey.

High concentration of D-Cu near sea surface

In this study, high D-Cu concentrations were observed at 5 and 10 m at Stn. 5 and at 5 m at Stn. 22. High concentrations of D-Cu near the sea surface have been reported, which are attributed to D-Cu supply by aerosol deposition or contamination from ships (BOYLE *et al.*, 1977; COALE and BRULAND, 1990; EZOE *et al.*, 2004). At the very least, the sample collected from 5 m at Stn. 22 is suspected to be contaminated because the concentration here (10.1 nmol l^{-1}, eliminated from figures) is an order of magnitude higher than previously reported values in the open ocean and because aerosol was sparse at this station (data not shown). Although the sampling side of the ship was toward the wind during sampling to avoid contamination from exhaust gas, completely avoiding contamination, at least for Cu, in samples taken near surface waters by a rosette sampler is difficult (BRULAND, 1980). On the contrary, the high D-Cu near the surface at Stn. 5 was at a level that has been explained by aerosol deposition or horizontal transport in previous reports (BOYLE *et al.*, 1977, 1981). In addition, from the surface to 12 m depth at Stn. 5, the salinity was lower (32.6–32.9) than that of the

Subarctic Upper Water (32.9–33.1) (Fig. 2c). Since low-salinity surface water was observed in large areas between 160° E and 180° in the north of 44.5° N during the cruise (Fig. 4), it is more likely to have been caused by a water mass, influenced by coastal supply, that was probably horizontally transported by the East Kamchatka Current (Favorite *et al.*, 1976), and not by precipitation. However, it is also possible that Cu was loaded by aerosol deposition onto the low-salinity surface water during its horizontal transport. D-Cu supply by the horizontal transport of the low-salinity surface water seems plausible because a high D-Cu concentration was observed in the low-salinity water (<12 m).

Comparison of D-Cu profile in the North Pacific

D-Cu vertical profiles in the eastern and western North Pacific, including both subarctic and subtropical areas, were compiled from the present and previous studies (Bruland, 1980; Buck *et al.*, 2012; Coale and Bruland, 1990; Ezoe *et al.*, 2004; Fujishima *et al.*, 2001; Hirose *et al.*, 1982; Midorikawa *et al.*, 1990; Miller and Bruland, 1994; Moffett and Dupont, 2007; Semeniuk *et al.*, 2009; Takano *et al.*, 2014) (Fig. 8). Here, values of Moffett and Dupont (2007) were read from figures. The D-Cu concentration at depths shallower than 1500 m at Stn. 5 vs. that of the compiled data without the data of Stn. 5 in this study and of Moffett and Dupont (2007) was 2.23–4.52 nM vs. 0.46–2.94 nM (0.94–2.56 nM higher than average of the values at other stations), and remained at almost the same level below 2000 m (Fig. 8). Moffett and Dupont (2007) also reported similarly high concentration of D-Cu between 500–1500 m in the subarctic North Pacific. However, these high values (2.35–4.52 nM) are not unrealistic, since the complexing capacity of organic ligand in the subarctic Pacific (generally ~3–4 nM, Coale and Bruland, 1990; Miller and Bruland, 1994; Moffet and Dupont,
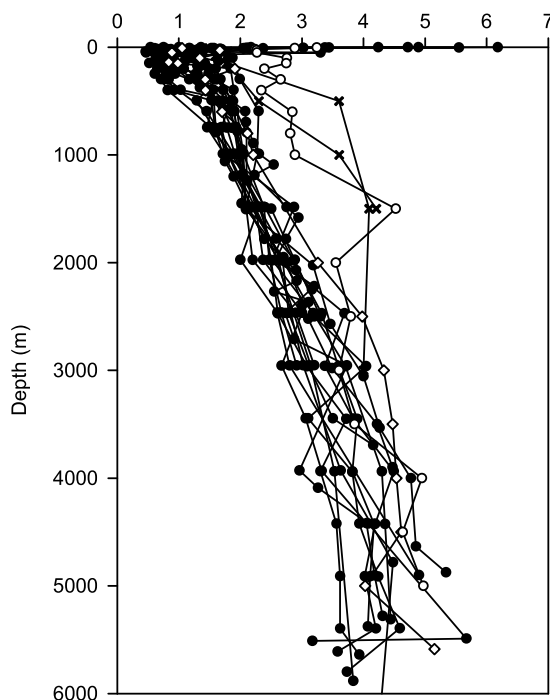

Fig. 8 Compiled data of vertical profile of D-Cu in previous studies in the Pacific Ocean (filled circle, Bruland, 1980; Buck *et al.*, 2012; Coale and Bruland, 1990; Ezoe *et al.*, 2004; Fujishima *et al.*, 2001; Hirose *et al.*, 1982; Midorikawa *et al.*, 1990; Miller and Bruland, 1994; Semeniuk *et al.*, 2009; Takano *et al.*, 2014: cross, Moffett and Dupont, 2007) and in this study (Stn. 5: open circle, Stn. 22: open diamond). Unit of nmol kg^{-1} in Takano *et al.* (2014) was converted into nmol l^{-1} using 1.02 kg l^{-1} as seawater density.

2007) is even higher than or at the same level as these values. To account for the high D-Cu concentration, it is necessary to consider supply and removal processes.

Sources and sinks of D-Cu in the euphotic layer

Within the euphotic layer, which is reported to be around 45–60 m in the western subarctic gyre (Mochizuki *et al.*, 2002; Tsuda *et al.*, 2005), aerosol deposition is an important source of Cu (Paytan *et al.*, 2009). Paytan *et al.* (2009) estimated

atmospheric deposition of Cu to be high in the western North Pacific, especially around 35–45° N, which is similar to the pattern of dust deposition estimates by other studies (UEMATSU et al., 2003; MEASURES et al., 2005). Although station BO01 (39°59′ N, 160°00′ E; June 23–24, 2000) of EZOE et al. (2004) is located closer to the center of the high Cu deposition region described above than Stn. 5 in the present study, the surface D-Cu concentration there was lower than that at Stn. 5. Moreover, the monthly averaged aerosol optical thickness at 550 nm as monitored by MODIS-Terra (Jul 2000) and MODIS-Aqua (Aug 2008) and produced with the Giovanni online data system at a website of the Goddard Earth Sciences Data and Information Services Center (GES DISC), showed higher aerosol density at station BO01 (0.157, Jul 2000) than at Stn. 5 (0.143, Aug 2008) at each sampling time. Additionally, in the Atlantic Ocean, the surface D-Cu distribution (BOYLE et al., 1981) was clearly different from that of D-Fe, which was covaried with dust deposition on a latitudinal transect (MOORE et al., 2009). Therefore, it is unlikely that dust deposition was the main cause of the high D-Cu concentration at Stn. 5, and it is necessary to consider other supply processes.

Another possible source of D-Cu into the euphotic layer is the transport of coastal water by horizontal advection (YEATS and CAMPBELL, 1983). There are two lines of evidence that show D-Cu supply by horizontal advection at Stn. 5. First, low-salinity water was observed at the surface around Stn. 5 as described above, which suggests horizontal advection of coastal water. Second, a satellite image of monthly-averaged surface Chl. a during August 2008, monitored by SeaWiFS (9 km) and produced with the Giovanni online data system, showed that high Chl. a water extends from the coast to large oceanic areas, around Stn. 5 (Fig. 9). Therefore, horizontal transport of
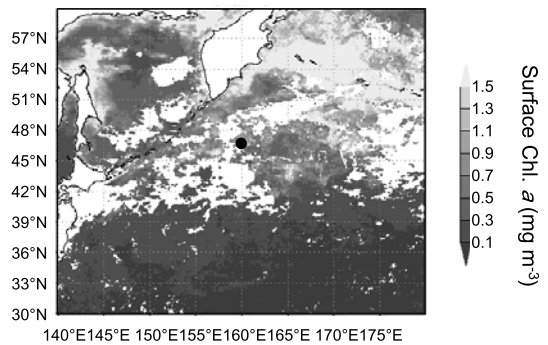

Fig. 9 Satellite images of surface Chl. a concentration during August 2008. Monthly averaged SeaWiFS 9 km data were depicted with Giovanni online data system (http://disc.sci.gsfc.nasa.gov/giovanni). Locations of Stn. 5 of this study were shown as dots on the map.

coastal water, rather than aerosol deposition, is considered to have been the main cause of the high D-Cu concentration at Stn. 5, although aerosol deposition could have also contributed to the Cu supply to some extent. Cu supply into the surface layer at Stn. 5 was also implied from Cu-Si relationship. Comparing D-Cu concentrations at same silicic acid concentration between 15–80 μmol 1^{-1}, they were approximately 0.6–1.8 nmol 1^{-1} higher at Stn. 5 than that at Stn. 22 (Figs. 7a and b). Therefore, Cu supply from atmosphere or coastal water was considered to raise D-Cu concentration near the sea surface.

The removal of D-Cu in the euphotic zone is mainly driven by biological consumption as shown by its nutrient-type profile. Primary production in the western subarctic North Pacific has been reported to be higher than in the tropical region (NORIKI et al., 1995; YAMADA et al., 2012). Moreover, surface Chl. a at Stn. 5 was relatively high in the western subarctic North Pacific. Although Fe could have been supplied with the transport of the coastal water, the high nitrate concentration in the surface water at Stn.

Table 1. Phytoplankton pigment composition at each depth was shown in $\mu g \, l^{-1}$.

Station	Depth	Chl c_3	Chld a	Peri	But	Fuco	Neo	Pras	Hex	Diad	Allo	Zea	Chl b	DV Chl a	MV Chl a
5	5	0.063	0.025	0.021	0.046	0.123	0.008	0.007	0.171	0.052	0.017	0.018	0.049	0	0.556
	10	0.061	0.017	0.016	0.045	0.114	0.008	0.008	0.172	0.044	0.011	0.013	0.053	0	0.472
	20	0.082	0.014	0.013	0.063	0.117	0.01	0.005	0.191	0.035	0.007	0.006	0.034	0	0.425
	30	0.091	0.01	0.01	0.074	0.151	0.012	0.017	0.147	0.024	0.008	0.009	0.054	0	0.48
	50	0.061	0	0	0.04	0.14	0.016	0.032	0.038	0.011	0.014	0.006	0.119	0	0.474
22	5	0	0	0.001	0.002	0.002	0	0	0.006	0.003	0	0.032	0.004	0.017	0.027
	10	0.001	0	0.002	0.002	0.003	0	0	0.009	0.004	0	0.032	0.005	0.017	0.051
	30	0.001	0	0.002	0.002	0.004	0	0	0.009	0.003	0	0.031	0.006	0.016	0.036
	50	0.003	0	0.003	0.003	0.005	0	0	0.012	0.004	0	0.044	0.007	0.028	0.044
	100	0.006	0	0.004	0.008	0.003	0.001	0	0.026	0.004	0	0.05	0.024	0.075	0.073
	140	0.024	0	0.002	0.037	0.004	0.002	0.001	0.005	0.003	0.001	0.034	0.15	0.136	0.106
	150	0.022	0	0.001	0.033	0.003	0.002	0.001	0.043	0.003	0.001	0.021	0.12	0.095	0.097
	200	0.008	0	0	0.01	0.001	0	0	0.014	0.001	0	0.002	0.029	0.013	0.03

Chl c_3: chlorophyll c_3, Chld a: chlorophyllide a, Peri: peridinin, But: 19´-butanoyloxyfucoxanthin, Fuco: fucoxanthin, Neo: neoxanthin, Pras: prasinoxanthin, Hex: 19´-hexanoyloxyfucoxanthin, Diad: diadinoxanthin, Allo: alloxanthin, Zea: zeaxanthin, Chl b: chlorophyll b, DV Chl a: divinyl chlorophyll a, MV Chl a: monovinyl chlorophyll a

5 (Fig. 6) implies that the station is located in a high-nitrate low-chlorophyll region, where primary production is limited by iron deficiency. Under such environments, some oceanic diatoms could replace Fe-containing enzymes with Cu-containing enzymes (PEERS and PRICE, 2006) and utilize multicopper oxidase for uptake of organically complexed Fe (ANNETT *et al.*, 2008; MALDONADO *et al.*, 2006), which could enhance the biological utilization of Cu by phytoplankton. Therefore, removal of D-Cu in the surface layer is considered to have been larger in the subarctic region than in the tropical region. Thus, supply process is probably responsible for the high concentration of D-Cu observed at Stn. 5.

Sources and sinks of D-Cu below the euphotic layer

Below the euphotic layer, one of the sources of D-Cu is regeneration accompanied by decomposition of sinking particles transported from the euphotic layer by the biological pump. As discussed above, the biological uptake of Cu at Stn. 5 is expected to have been relatively high. Thus, the supply of Cu by regeneration in the deeper layer is estimated to have been higher in this region than that in the other regions. However, below 2000 m, there was no discernible difference in D-Cu concentrations between Stn. 5 and the other stations (Fig. 8). This is probably because the organic matter was almost fully decomposed around this depth.

Supply of D-Cu by deep sea circulation is also possible to be a cause of high D-Cu above 1500 m at Stn. 5. The subarctic North Pacific is an end region of deep sea circulation, where the deeper water is upwelling with high D-Cu. As described above, MOFFETT and DUPONT (2007) also reported high D-Cu concentration between 500–1500 m in the subarctic North Pacific. Therefore, such a supply process of D-Cu is possible. However, values reported by TAKANO *et al.* (2014) in the

western subarctic north Pacific were not as high as those observed at Stn. 5 in this study. Thus, concentration of D-Cu may be spatially or temporally variable in this region.

Another supply process of Cu in deeper layers is transport by horizontal advection. To evaluate Cu sources other than the biological pump of diatoms, vertical profiles of the D-Cu:silicic acid (Cu:Si) ratio at Stns. 5 and 22 were plotted (Fig. 10). The ratio at Stn. 5 was highest (2.1) at the surface, had its minimum (0.019) at a 1000 m depth, and then slightly increased toward the bottom (0.035). The high Cu:Si ratio near the surface was caused by biological Si consumption and relatively high Cu at the surface. On the contrary, the high Cu:Si ratio near the bottom can be explained by Cu supply from bottom sources and a decrease in silicic acid below the Si maximum. Profiles of the Cu:Si ratio at both stations ranged within the same level (approximately 0.02–0.03) between 400 and 2000 m, suggesting that Cu and Si were mainly controlled by the biological pump by diatoms in this depth range along the advection pathway of water masses in this layer. However, a slightly high ratio was observed at 1500 m at Stn. 5, which corresponded to a high concentration of D-Cu
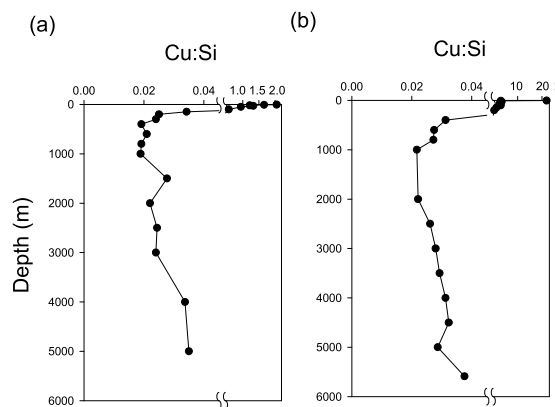

Fig. 10   Vertical profiles of Cu:Si ratio at Stns. 5 (a) and 22 (b).

(4.52 nM). To this region, Fe is supplied by horizontal advection of water mass from the Sea of Okhotsk, which contains high dissolved-Fe. This water mass is characterized by σ_θ of 26.6–27.5 (NISHIOKA *et al.*, 2007), which corresponds to 116–1110 m at Stn. 5. Therefore, the horizontal advection of this water mass cannot explain the D-Cu concentration anomaly at 1500 m. However, it is possible that this process supplied D-Cu between 116–1110 m at Stn. 5 although no apparent signal of the supply was observed in the D-Cu profile and the Cu:Si plot at this station.

Considering the high sinking particle flux in the western subarctic North Pacific (NORIKI *et al.*, 1995; KAWAHATA, 2002), removal by scavenging is likely to have also been high. Thus, the supply of D-Cu is considered to have been high enough to sustain the high D-Cu concentration, compensating for its high removal in the euphotic zone (biological uptake) and below (scavenging).

Comparison with Ni

Among the trace metal elements, the distribution pattern of dissolved nickel (Ni) was similar to that of D-Cu in the point of view that it was higher in the subarctic North Pacific than in the subtropical above the maximum at around 1500 m, and almost no regional variation was observed below the maximum (EZOE *et al.*, 2004). Nickel showed a nutrient-type profile that frequently correlated with phosphate and silicic acid (BRULAND 1980; BOYLE *et al.*, 1981), which implies the importance of control by the biological pump, related to diatoms, on both Cu and Ni distributions.

Future directions

In the present study, vertical profiles of D-Cu were examined at the western North subarctic and tropical stations, together with other hydrographic and biological parameters. This study presents high D-Cu concentrations in the western subarctic North Pacific. Our results suggest that

Cu was supplied to the surface layer of the western subarctic North Pacific primarily by horizontal advection and, to a lesser extent, by aerosol deposition. The Cu was then transported downward through the biological pump to a depth of 1500 m. Moreover, a direct supply of Cu to the same depth by horizontal advection is also implied, although the source of the water mass and mechanism of the advection are unclear. More detailed observation is necessary to elucidate them in the future. The present study also suggests that the biological pump is the main source of Cu in the middle layer in the western subarctic North Pacific. Therefore, it is important to determine the amount of Cu utilized by microbes and the amount of Cu supporting primary production in the Fe-depleted region as this will enable us to further understand the Cu transport process. Furthermore, it is important to understand the effect of changes in aerosol deposition accompanied by future climate change on Cu concentration in the natural environment, because change of Fe supply from dust affects Fe deficiency of ocean surface and thus Cu requirement of phytoplankton and accordingly downward flux of Cu by biological pump.

References

ANNETT, A.L., S. LAPI, T.J. RUTH, and M.T. MALDONADO

(2008): The effects of Cu and Fe availability on the growth and Cu:C ratios of marine diatoms. Limnol. Oceanogr. **53**, 2451-2461.

BOYE, M., B.D. WAKE, P. LOPEZ GARCIA, J. BOWN, A. R. BAKER, and E.P. ACHTERBERG (2012): Distributions of dissolved trace metals (Cd, Cu, Mn, Pb, Ag) in the southeastern Atlantic and the Southern Ocean. Biogeosciences **9**, 3231-3246.

BOYLE, E. A., F. R. SCLATER, and J. M. EDMOND (1977): The distribution of dissolved copper in the Pacific. Earth Planet. Sci. Lett. **37**, 38-54.

BOYLE, E. A., S. S. HUESTED, and S. P. JONES (1981): On the distribution of copper, nickel, and cadmium in the surface waters of the North Atlantic and North Pacific Ocean. J. Geophys. Res. **86**, 8048-8066.

BRULAND, K.W. (1980): Oceanographic distributions of cadmium, zinc, nickel, and copper in the North Pacific. Earth Planet. Sci. Lett. **47**, 176-198.

BUCK, K.N., J. MOFFETT, K.A. BARBEAU, R.M. BUNDY, Y. KONDO, and J. WU (2012): The organic complexation of iron and copper: an intercomparison of competitive ligand exchange-adsorptive cathodic stripping voltammetry (CLE-ACSV) techniques. Limnol. Oceanogr. **10**, 496-515.

CAMPOS, M.L.A.M., and C.M.G. VAN DEN BERG (1994): Determination of copper complexation in sea water by cathodic stripping voltammetry and ligand competition with salicylaldoxime. Anal. Chim. Acta **284**, 481-496.

COALE, K. H. (1991): Effects of iron, manganese, copper, and zinc enrichments on productivity and biomass in the subarctic Pacific. Limnol. Oceanogr. **36**, 1851-1864.

COALE, K.H., and K.W. BRULAND (1990): Spatial and temporal variability in copper complexation in the North Pacific. Deep-Sea Res. **37**, 317-336.

DANIELSSON, L. G. (1980): Cadmium, cobalt, copper, iron, lead, nickel and zinc in Indian Ocean water. Mar. Chem. **8**, 199-215.

DANIELSSON, L.G., B. MAGNUSSON, and S. WESTERLUND (1985): Cadmium, copper, iron, nickel and zinc in the north-east Atlantic Ocean. Mar. Chem. **17**, 23-41.

EZOE, M., T. ISHITA, M. KINUGASA, X. LAI, K. NORISUYE,

and Y. SOHRIN (2004): Distributions of dissolved and acid-dissolvable bioactive trace metals in the North Pacific Ocean. Geochem. J. **38**, 535-550.

FAVORITE, F., A. J. DODIMEAD, and K. NASU (1976): Oceanography of the subarctic pacific region, 1960-71. Bulletin of the International North Pacific Fishery Commission. **33**, 1-187.

FEELY, R.A., C.L. SABINE, R. SCHLITZER, J.L. BULLISTER, S. MECKING, and D. GREELEY (2004): Oxygen utilization and organic carbon remineralization in the upper water column of the Pacific Ocean. J. Oceanogr. **60**, 45-52.

FUJISHIMA, Y., K. UEDA, M. MARUO, E. NAKAYAMA, C. TOKUTOME, H. HASEGAWA, M. MA and Y. SOHRIN (2001): Distribution of trace bioelements in the subarctic North Pacific Ocean and the Bering Sea (the R/V Hakuho Maru Cruise KH-97-2). J. Oceanogr. **57**, 261-273.

FURUYA, K., M. HAYASHI, Y. YABUSHITA, and A. ISHIKAWA (2003): Phytoplankton dynamics in the East China Sea in spring and summer as revealed by HPLC-derived pigment signatures. Deep-Sea Res. Pt. II **50**, 367-387.

GRASSHOFF, K., K. KREMING, and M. EHRHARDT (1999): Methods of Seawater Analysis, Willey-VCH, 3rd edition, 632pp.

HIROSE, K., Y. DOKIYA, and Y. SUGIMURA (1982): Determination of conditional stability constants of organic copper and zinc complexes dissolved in seawater using ligand exchange method with EDTA. Mar. Chem. **11**, 343-354.

KAWAHATA, H. (2002): Suspended and settling particles in the Pacific. Deep-Sea Res. Pt. II **49**, 5647-5664.

KINUGASA, M., T. ISHITA, Y. SOHRIN, K. OKAMURA, S. TAKEDA, J. NISHIOKA, and A. TSUDA (2005): Dynamics of trace metals during the subarctic Pacific iron experiment for ecosystem dynamics study (SEEDS2001). Prog. Oceanogr. **64**, 129-147.

KONDO, Y., S. TAKEDA, and K. FURUYA (2012): Distinct trends in dissolved Fe speciation between shallow and deep waters in the Pacific Ocean. Mar. Chem. **134-135**, 18-28.

LÖSCHER, B.M. (1999): Relationships among Ni, Cu, Zn, and major nutrients in the Southern Ocean. Mar.

Chem. **67**, 67–102.

MALDONADO, M.T., A.E. ALLEN, J.S. CHONG, K. LIN, D. LEUS, N. KARPENKO, and S.L. HARRIS (2006): Copper-dependent iron transport in coastal and oceanic diatoms. Limnol. Oceanogr. **51**, 1729–1743.

MANN, E.L., N. AHLGREN, J.W. MOFFETT, and S.W. CHISHOLM (2002): Copper toxicity and cyanobacteria ecology in the Sargasso Sea. Limnol. Oceanogr. **47**, 976–988.

Martin, J. M., and M. Whitfield (1983): The significance of the river input of chemical elements to the ocean. *In* Trace Metals in Sea Water. WONG, C. S., E. BOYLE, K. W. BRULAND, J. D. BURTON and E. D. GOLDBERG (eds.), Plenum Press, New York and London, p. 265–296

MEASURES, C.I., M.T. BROWN, and S. VINK (2005): Dust deposition to the surface waters of the western and central North Pacific inferred from surface water dissolved aluminum concentrations. Geochemistry, Geophys. Geosystems **6**.

MIDORIKAWA, T., E. TANOUE, and Y. SUGIMURA (1990): Determination of complexing ability of natural ligands in seawater for various metal ions using ion selective electrodes. Anal. Chem. **62**, 1737–1746.

MIKI, M., N. RAMAIAH, S. TAKEDA, and K. FURUYA (2008): Phytoplankton dynamics associated with the monsoon in the Sulu Sea as revealed by pigment signature. J. Oceanogr. **64**, 663–673.

MILLARD, R., W. OWENS, and N. FOFONOFF (1990): On the calculation of the Brunt-Väisälä frequency. Deep-Sea Res. **37**, 167–181.

MILLER, L.A., and K.W. BRULAND (1994): Determination of copper speciation in marine waters by competitive ligand equilibration/liquid-liquid extraction: an evaluation of the technique. Anal. Chim. Acta **284**, 573–586.

MOCHIZUKI, M., N. SHIGA, M. SAITO, K. IMAI, and Y. NOJIRI (2002): Seasonal changes in nutrients, chlorophyll *a* and the phytoplankton assemblage of the western subarctic gyre in the Pacific Ocean. Deep-Sea Res. Pt. II **49**, 5421–5439

MOFFETT, J.W., L.E. BRAND, P.L. CROOT, and K.A. BARBEAU (1997): Cu speciation and cyanobacterial distribution in harbors subject to anthropogenic Cu inputs. Limnol. Oceanogr. **42**, 789–799.

MOFFETT, J.W., and C. DUPONT (2007): Cu complexation by organic ligands in the sub-arctic NW Pacific and Bering Sea. Deep-Sea Res. Pt. I **54**, 586–595.

MOORE, R.M. (1978): The distribution of dissolved copper in the eastern Atlantic Ocean. Earth Planet. Sci. Lett. **41**, 461–468.

MOORE, J.K., and O. BRAUCHER (2008): Sedimentary and mineral dust sources of dissolved iron to the world ocean. Biogeosciences **5**, 631–656.

MOORE, C.M., M.M. MILLS, E.P. ACHTERBERG, R.J. GEIDER, J. LAROCHE, M.I. LUCAS, E.L. MCDONAGH, X. PAN, A.J. POULTON, M. J. A. RIJKENBERG, D. J. SUGGETT, S. J. USSHER, and E.M.S. WOODWARD (2009): Large-scale distribution of Atlantic nitrogen fixation controlled by iron availability. Nat. Geosci. **2**, 867–871.

NISHIOKA, J., T. ONO, H. SAITO, T. NAKATSUKA, S. TAKEDA, T. YOSHIMURA, K. SUZUKI, K. KUMA, S. NAKABAYASHI, D. TSUMUNE, H. MITSUDERA, W.K. JOHNSON, and A. TSUDA (2007): Iron supply to the western subarctic Pacific: Importance of iron export from the Sea of Okhotsk. J. Geophys. Res. **112**, C10012

NOLTING, R.F., H.J.W. DE BAAR, A.J. VAN BENNEKOM, and A. MASSON (1991): Cadmium, copper and iron in the Scotia Sea, Weddell Sea and Weddell/Scotia Confluence (Antarctica). Mar. Chem. **35**, 219–243.

NORIKI, S., T. IWAI, A. SHIMAMOTO, S. TSUNOGAI, and K. HARADA (1995): Spatial variation of Al flux in the North Pacific observed with sediment trap. *In* Biogeochemical Processes and Ocean Flux in the Western Pacific. SAKAI H. and Y. NOZAKI (eds.), Terra Scientific Publishing Company, Tokyo, p. 345–354.

PAYTAN, A., K.R.M. MACKEY, Y. CHEN, I.D. LIMA, S.C. DONEY, N. MAHOWALD, R. LABIOSA, and A.F. POST (2009): Toxicity of atmospheric aerosols on marine phytoplankton. Proc. Natl. Acad. Sci. U. S. A. **106**, 4601–4605.

PEERS, G., and N.M. PRICE (2006): Copper-containing plastocyanin used for electron transport by an oceanic diatom. Nature **441**, 341–344.

SAAGER, P. M., H. J. W. DE BAAR, and R. J. HOWLAND. (1992): Cd, Zn, Ni and Cu in the Indian Ocean.

Deep-Sea Res. **39**, 9–35.

SAAGER, P. M., H. J. W. DE BAAR, J. T. M. DE JONG, R. F. NOLTING, and J. SCHIJF (1997): Hydrography and local sources of dissolved trace metals Mn, Ni, Cu, and Cd in the northeast Atlantic Ocean. Mar. Chem. **57**, 195–216.

SANDER, S. G., and A. KOSCHINSKY (2011): Metal flux from hydrothermal vents increased by organic complexation. Nat. Geosci. **4**, 145–150.

SCHLITZER, R., Ocean Data View, http://odv.awi.de, 2012.

SEMENIUK, D. M., J. T. CULLEN, W. K. JOHNSON, K. GAGNON, T. J. RUTH, and M. T. MALDONADO (2009): Plankton copper requirements and uptake in the subarctic Northeast Pacific Ocean. Deep Sea Res. Pt. I **56**, 1130–1142.

SOARES, H. M. V. M., and M. G. R. T. BARROS (2001): Electrochemical Processes of cadmium, copper, lead, and zinc in the presence of *N*-(2-hydroxyethyl) piperazine-*N*'-3-propanesulfonic acid (HEPPS): Possible implications in speciation studies. Electroanalysis **13**, 325–331.

SUGA, T., A. KATO, and K. HANAWA (2000): North Pacific Tropical Water: its climatology and temporal changes associated with the climate regime shift in the 1970s. Prog. Oceanogr. **47**, 223–256.

SUGA, T., K. MOTOKI, Y. AOKI, and A. M. MACDONALD (2004): The North Pacific climatology of winter mixed layer and mode waters. J. Phys. Oceanogr. **34**, 3–22.

TAKANO, S., M. TANIMIZU, T. HIRATA, and Y. SOHRIN (2014): Isotopic constraints on biogeochemical cycling of copper in the ocean. Nat. Commun. **5**, 5663.

TOMCZAK, M., and J. S. GODFREY (2005): Regional Oceanography: an Introduction, pdf version 1.1, Butler and Tanner Ltd, London, 391pp.

TSUDA, A., H. KIYOSAWA, A. KUWATA, M. MOCHIZUKI, N. SHIGA, H. SAITO, S. CHIBA, K. IMAI, J. NISHIOKA, and T. ONO (2005): Responses of diatoms to iron-enrichment (SEEDS) in the western subarctic Pacific, temporal and spatial comparisons. Prog. Oceanogr. **64**, 189–205.

TWINING, B., and S. BAINES (2013): The trace metal composition of marine phytoplankton. Ann. Rev. Mar. Sci. **5**, 191–215.

UEMATSU, M., Z. F. WANG, and I. UNO (2003): Atmospheric input of mineral dust to the western North Pacific region based on direct measurements and a regional chemical transport model. Geophys. Res. Lett. **30**, 1342

WEISS, R. F. (1970): The solubility of nitrogen, oxygen and argon in water and seawater. Deep-Sea Res. **17**, 721–735.

WESTERLUND, S., and P. ÖHMAN (1991): Cadmium, copper, cobalt, nickel, lead, and zinc in the water column of the Weddell Sea, Antarctica. Geochim. Cosmochim. Acta **55**, 2127–2146.

YAMADA, N., H. FUKUDA, H. OGAWA, H. SAITO, and M. SUZUMURA (2012): Heterotrophic bacterial production and extracellular enzymatic activity in sinking particulate matter in the western North Pacific Ocean. Front. Microbiol. **3**, 379.

YEATS, P. A., and J. A. CAMPBELL (1983): Nickel, copper, cadmium and zinc in the northwest Atlantic Ocean. Mar. Chem. **12**, 43–58.

ZAPATA, M., F. RODRÍGUEZ, and J. GARRIDO (2000): Separation of chlorophylls and carotenoids from marine phytoplankton:a new HPLC method using a reversed phase C8 column and pyridine-containing mobile phases. Mar. Ecol. Prog. Ser. **195**, 29–45.

沿岸域におけるサルパ・ブルームと有機物の鉛直輸送

深尾剛志[1]＊・朝日俊雅[1]・多田邦尚[1]

Salp bloom and vertical fluxes of organic matter in coastal water

Tsuyoshi FUKAO, Toshimasa ASAHI and Kuninao TADA

Abstract: The changes of salp abundance and environmental factors such as water temperature and salinity were investigated in surface water of Shitaba Bay, Uwa Sea, Japan, in spring, 2011. Furthermore, sediment trap samples were collected at the bottom ocean layer of Shitaba Bay during salp bloom phase or non-bloom phase. Maximum salp abundance were recorded at 26 April, but no salp were observed at water temperatures of more than 20℃ (from 12 May onwards). Particulate organic carbon and nitrogen fluxes during salp bloom phase were higher than those during non-bloom phase. Therefore, these results showed that salp bloom in spring contributed to rapid supply of particulate organic matter from surface to bottom layer in coastal environments.

Keywords: salp bloom, water temperature, sediment trap, organic matter flux

1. はじめに

　サルパ類は，脊索動物門，被囊動物亜門，タリア綱に属し，クラゲと同様にゼラチン質の体をもつ動物プランクトンであり，主に外洋域に生息している（西川, 2001, 2003 ）．サルパ類は，無性生殖を行う単独個体（solitary zooid）と雌雄同体で有性生殖を行う連鎖個体（aggregate zooid）の2種類の形態が存在し，交互に世代交代を繰り返す（西川, 2003）．近年，春季の日本海を中心にサルパの大量発生（以後,「サルパ・ブルーム」と記す）が報告され，刺網や定置網に付着することで漁労作業に支障を来していることが報告されている

1）香川大学農学部
　〒 761-0795　香川県木田郡三木町池戸 2393
　＊連絡先 E-mail: fukao@water.ocn.ne.jp
　Tel./Fax＋81-87-891-3148

（黒田ら, 2000; 藤井, 2007; 飯田, 2009）．また敦賀原子力発電所では，取水口に 5cm 程のトガリサルパ（*Salpa fusiformis*）が大量侵入し，復水器系統のフィルターを詰まらせた結果，1ヶ月近く発電出力を 40% まで低下させる被害を被っている（藤井, 2007）．一方で，サルパはマサバをはじめとした魚類に捕食されていることから生態系の一端を担っていることが明らかとなっている（西村, 1958; 飯田, 2009）．サルパ・ブルームの出現に関する記録は愛媛県宇和海沿岸においても報告されている（森実, 1995）．1994 年 4 月にはトガリサルパが大量発生し，養殖ハマチの鰓把をサルパが覆って鰓への通水を阻害した結果ハマチの窒息死を引き起こした（森実, 1995）．それ以降もほぼ毎年 4 月ごろからサルパ・ブルームの形成がみられることから，漁業被害を避けるためにもその発生機構を明らかにすることは重要であると考えられ

る．サルパの分布・生態に関する研究は主に外洋域が中心であり（Iseki, 1981; Madin, 1982; Nishikawa et al., 1995; Nishikawa and Tsuda, 2001; Iguchi and Ikeda, 2004; Ono et al., 2010），沿岸域におけるサルパ・ブルームの形成に関する詳細な条件等は未だに明らかにされていないのが現状である．さらに，サルパは大量の植物プランクトンや植食性動物プランクトンを含む懸濁物をろ過し懸濁物を凝集した糞を排出することから（西川, 2001, 2003），貧栄養である外洋域において高密度のブルームが発生した場合，ブルーム発生海域表層の懸濁物が大量に摂食され，排出された糞が素早い有機物の鉛直輸送に大きく寄与していることが報告されている（Iseki, 1981; Madin, 1982; Morris et al., 1988）．沿岸域であるにもかかわらず貧栄養の傾向を示す春季の宇和海において（山下ら, 2011），サルパ・ブルームが形成された場合も同様に大量のサルパ由来の有機物が底層に供給されているものと予想される．そこで本研究では，愛媛県の宇和海沿岸域の一つ下波湾の魚類養殖場において，2011 年春季に発生したサルパ・ブルームによる有機物の鉛直輸送への影響について明らかにすることを目的とした．

2．方法

2.1　調査定点

調査定点を Fig. 1 に示す．下波湾は宇和海東部の愛媛県宇和島市に位置し，湾口幅約 1.8 km，奥行き約 2.8 km，面積約 3 km^2，湾奥付近の水深は 20 m 程度，湾中央部から湾口にかけては水深 50-60 m の内湾であり，二級河川以上の河川の流入がない．本湾はタイやハマチを主体とした魚類養殖と真珠養殖が営まれている．調査は，下波湾の湾口部の愛媛県農林水産研究所水産研究センターの地先に設置されている魚類養殖筏 Stn. A（平均水深 25 m）で実施した．

2.2　サルパの個体数調査および環境因子の測定

サルパの個体数調査は，2011 年 4 月下旬から 6 月初旬にかけて平日は概ね毎日養殖生簀の上からポリエチレン製バケツで表層の海水 1〜10 L を採取した．海水は目開き 106 μm のふるいでろ過し，ふるい上のサルパについて単独個体と連鎖個体の合計個体数を肉眼で計数した．また，採水試料の違いによる個体数の偏りを防ぐため，十回の採水を行って計数し，その平均値をサルパの個体数とした．採集したサルパの一部は，予め強熱処理（450℃，3 時間）した GF/F フィルター（Whatman）でろ過した海水で洗浄した後，GF/F ろ過海水中
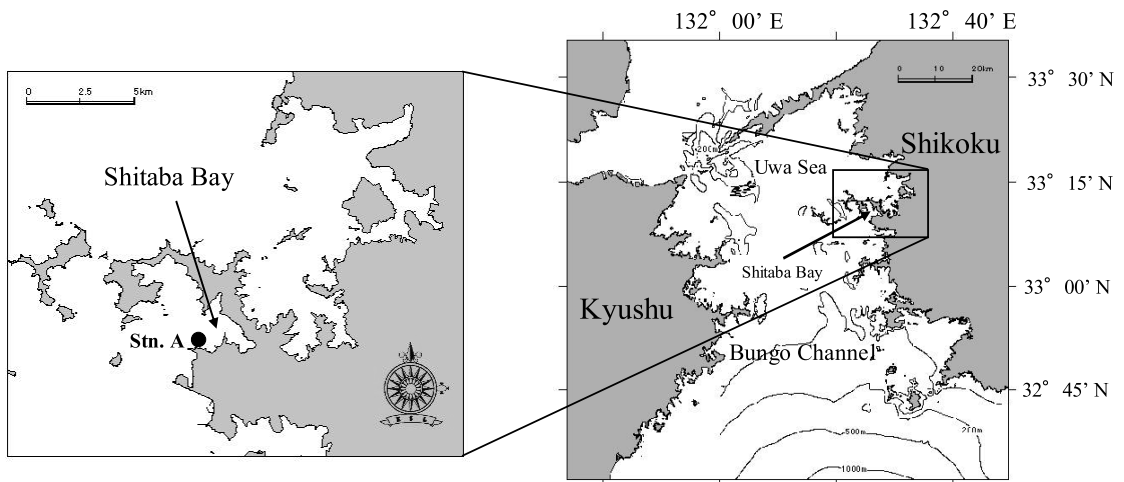

Fig. 1　Location of sampling station（Stn. A）in Shitaba Bay, Uwa Sea

で数時間飼育し糞を排出させた．サルパを除去
後，糞を含む海水は GF/F フィルター上にろ過捕
集した．サルパ本体と糞を捕集したフィルターは
それぞれ − 30 ℃中で凍結した後，凍結乾燥して
重量測定後，成分分析までデシケーター中で常温
保存した．調査定点表層水（0〜0.5 m）の水温お
よび塩分は多項目水質計（アレック電子株式会社，
クロロテック AAQ175）あるいは防水型デジタル
温度計（佐藤計量器製作所，SK-1250MCIII *a*）
により測定した．なお透明度および一部の水温
は，愛媛県農林水産研究所水産研究センターの
データを利用した．

2.3 沈降粒子の捕集実験

　サルパ・ブルーム時あるいは非サルパ・ブルー
ム時にセディメントトラップを設置し，沈降粒子
捕集実験を行った．実験には，アクリル製筒を 6
本装着した M 型トラップ（MONTANI *et al.*, 1988）
を行った．実験時，捕集された沈降粒子の筒内で
の舞い上がりを最小にするため，アクリル製筒の
底にプラスチック製のグリッドを置いた（多田ら，
2009）．トラップは，表層水中のサルパが混入し
ないようにするため陸上で筒の中を目開き 106
μm のふるいでろ過した海水で満たした後水深
15 m 層に沈め，養殖生簀から直接係留した（Fig.
2）．なお，実験期間中はトラップが設置されてい
る付近において魚類養殖は行われていない．ト
ラップを約 2 日間放置した後に回収し，6 本の内
4 本のトラップの筒を静置してサイフォンで上澄
液を取り除いた．筒中の沈降粒子は，GF/F フィ
ルター上にろ過捕集した．沈降粒子はろ過捕集完
了後，炭酸塩を除去するため 1M 塩酸処理を数分
施し，さらに塩酸が除去されるまで蒸留水で洗浄
しながらろ過を続けた．沈降粒子を捕集したフィ
ルターは − 30 ℃中で凍結した後凍結乾燥して重
量測定後成分分析までデシケーター中で常温保存
した．サルパ，サルパの糞および沈降粒子中の有
機態炭素・窒素量の分析は，CHN コーダー（J-
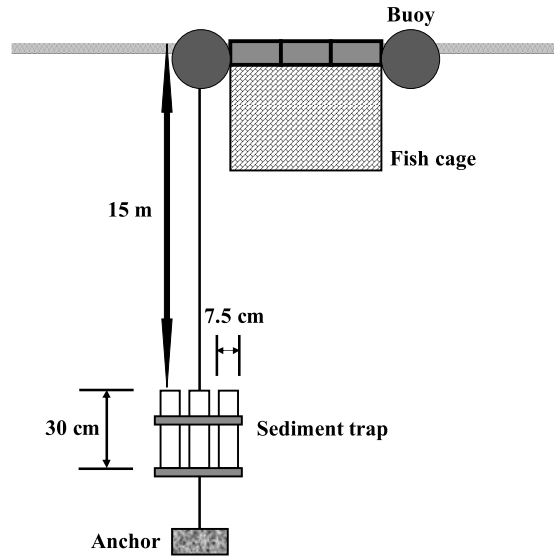SCIENCE LAB Co., Ltd., MICRO CORDER
JM10）を用いて測定した．

Fig. 2　Schematic diagram of sediment trap system

3. 結果および考察

3.1 サルパの変動とそれに及ぼす環境要因

　2011 年 4 月下旬から 5 月上旬にかけてサルパ
のブルームが観察された（Fig. 3）．4 月 26 日に
最大個体密度 18920 inds. m^{-3}に達し，その後約
2〜3 日程度でブルームの形成・消滅を繰り返し，
これが 5 月 11 日まで続いた（Fig. 3）．サルパの
体長が約 1〜3 cm であることと形態から過去に
宇和海沿岸を調査した森実（1995）の報告と同様
にトガリサルパであると判断した（Fig. 4a, b, c）．
ブルーム形成前に表層水中を単独個体が遊泳して
いるのが確認され，その数時間後大規模な連鎖個
体によるブルームが出現した（Fig. 4d）．またブ
ルームの衰退期には，サルパ以外にミズクラゲ
（*Aurelia aurita*）あるいは複数種のハコクラゲ属
（*Abyla* spp.）も多く確認することができた．サル
パ・ブルーム形成期間が終了する頃（5 月 8 日）に
続いて夜光虫（*Noctiluca scintillans*）赤潮が形成
される水域がパッチ状に増加していった．サル
パ・ブルーム消滅直後，粘性を有するサルパの死
骸や糞が凝集したヌタ（三島ら，1990）が浮遊し
ている海域も一部で確認できた（Fig. 4e）．サル
パは，体内の粘性を有する網で餌となる懸濁粒子
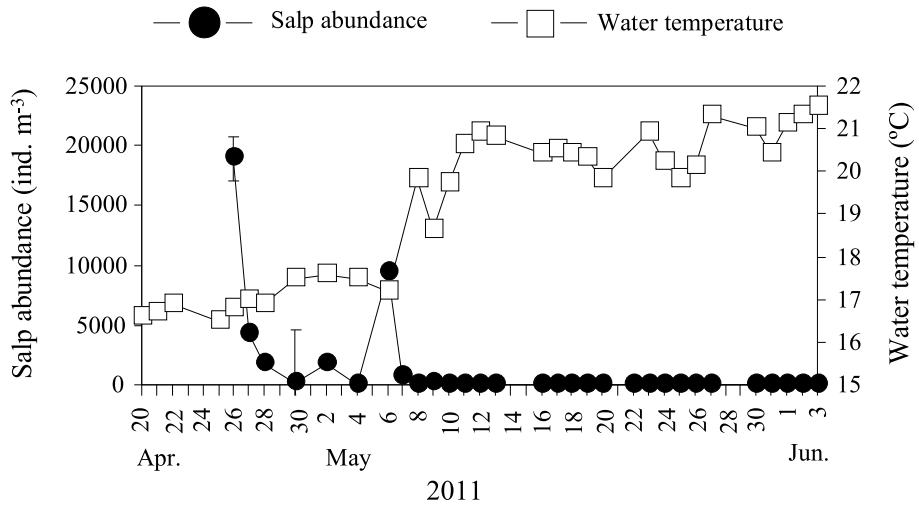を濾しとることが知られている（西川, 2001, 2003;

Fig. 3 Changes of salp abundance and water temperature in surface water (0–0.5 m) of Shitaba Bay from late April to early June, 2011. The error bars represent one standard deviation
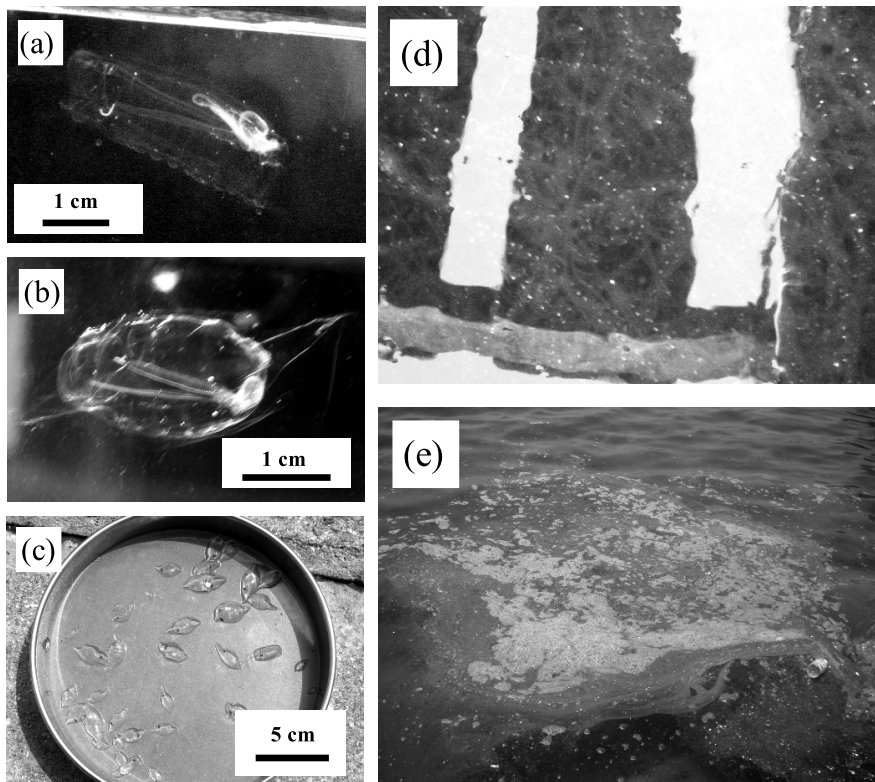

Fig. 4 Photographs of solitary zooid (a) and aggregate zooid (b) of salp *Salpa fusiformis*, salps collected in a sieve (c), salp bloom (d) and Nuta aggregates formed by salp cadaver (e)

BONE *et al.*, 2000）．ヌタは，サルパから放出された網にサルパの死骸や海水中の懸濁粒子が付着し凝集したものと考えられ，大規模に発生した場合養殖生簀の網等に付着することで水産業にダメージを与える可能性があり，沿岸域では今後注意が必要であると思われる．サルパ・ブルームは，水温が20℃以上になる5月11日を最後にみられなくなった（Fig. 3）．また，調査期間中の塩分（34.57～34.77）に著しい変動はなかった．トガリサルパがブルームのような高密度で出現する場合の最適水温の上限は，16.5～22℃の範囲にあると報告されていることから（BRACONNOT, 1971; LICANDRO *et al.*, 2006; CHAE *et al.*, 2008; LIU *et al.*, 2012; FRANCO *et al.*, 2014）今回の調査と概ね一致し，サルパ・ブルームが形成されなくなったのは水温の上昇によるものと考えられる．調査期間終了後も2012年3月まで表層水中を肉眼で監視し続けたが，12月から3月まで水温が20℃以下になったにもかかわらずサルパ・ブルームをみることがなかった．これは，冬の宇和海は強風の影響で海が荒れやすいため表層水中でサルパが遊泳できないものと推測され，ブルームが形成されるのは20℃以下かつ海がおだやかな春季の狭い期間に限られていると考えられる．また，サルパは水深50m以深にも生息していることから（MORRIS *et al.*, 1988; NISHIKAWA and TSUDA, 2001; PAGÈS *et al.*, 2001; ONO *et al.*, 2010），プランクトンネットを用いて底層（約15 m）におけるサルパの有無を調べたものの，やはり5月12日以降観察すること

はできなかった．これらのことから，サルパは下波湾に常在しているわけではなく，上層から黒潮系暖水が突発的に沿岸域に侵入する現象である急潮（武岡ら, 1992; 小泉, 2002）あるいは急潮後下層から陸棚斜面域由来の冷水が浸入する現象である底入り潮（小泉, 2002; 兼田ら, 2010）とともに外洋から移入してくると推測され，今後下波湾への侵入経路の特定が必要になるものと考えられる．

3.2 サルパ・ブルームによる沈降粒子束への影響

サルパ・ブルーム時（5月6日～8日）および非サルパ・ブルーム時（夜光虫赤潮：5月11日～13日および非ブルーム：5月17日～19日と5月24日～26日）にセディメントトラップで捕集したそれぞれの沈降物の特性は異なっていた．サルパ・ブルーム時の沈降物は，弱い粘性を有する白い膜状の物質で粒子が凝集した状態であったのに対し（Fig. 5a），夜光虫赤潮あるいは非ブルーム時のものは粒子が粉状に散けていた（Fig. 5b, c）．全沈降粒子フラックスは5.20-7.16 g dry m^{-2} day^{-1}の範囲であり，サルパ・ブルームの発生による有意な差異は認められなかった（Fig. 6, Tukey 法, $p >$ 0.05）．一方，有機炭素フラックスにおいて，サルパ・ブルーム時（0.31 g-C dry m^{-2} day^{-1}）と夜光虫赤潮時（0.29 g-C dry m^{-2} day^{-1}）は非ブルーム時（0.084 および 0.063 g-C dry m^{-2} day^{-1}）より有意に高かった（Fig. 7a, Tukey 法, $p <$ 0.01）．また有
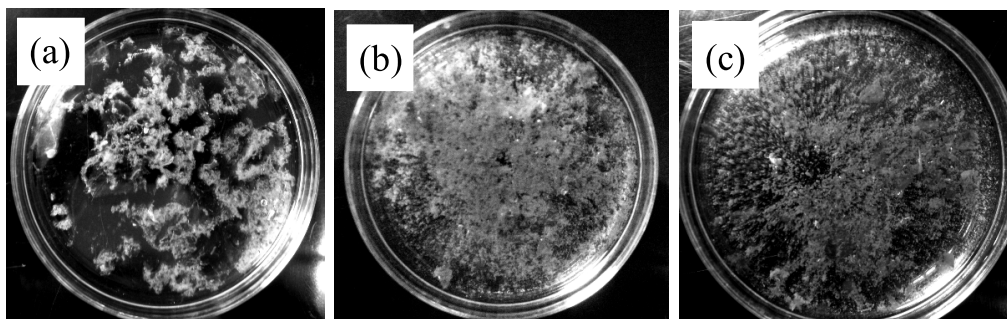

Fig. 5 Photographs of settling matter collected by sediment trap during salp bloom（a），*Noctiluca* red tide（b）and non-bloom（c）

機窒素フラックスにおいても同様に，サルパ・ブルーム時（0.061 g-N dry m^{-2} day^{-1}）と夜光虫赤潮時（0.049 g-N dry m^{-2} day^{-1}）は非ブルーム時（0.011および 0.0085 g-N dry m^{-2} day^{-1}）より有意に高かった（Fig. 7b, Tukey 法，$p < 0.01$）．全沈降粒子フラックスに有意差が生じなかった原因とし
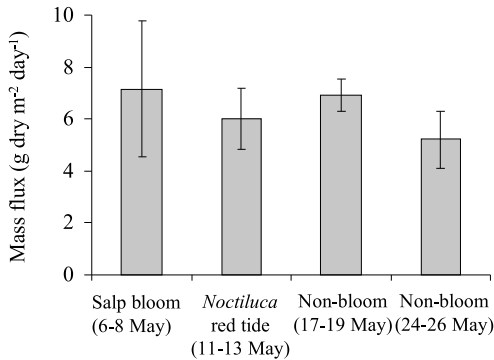

Fig. 6   Mass flux during salp bloom, *Noctiluca* red tide, and non-bloom. The error bars represent one standard deviation
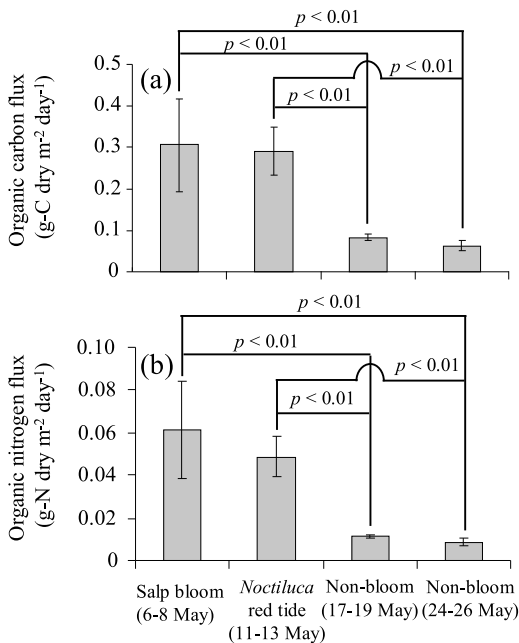

Fig. 7   Organic carbon flux（a）and organic nitrogen flux（b）during salp bloom, *Noctiluca* red tide, and non-bloom. The error bars represent one standard deviation

て，全沈降粒子フラックスに占める有機炭素フラックスおよび有機窒素フラックスの割合が，それぞれ 1.21–4.84% および 0.16–0.86% に過ぎなかったためと考えられる．サルパの体および糞に含まれる有機態の炭素量と窒素量も沈降物と同様に分析し，沈降物と比較した．サルパ・ブルーム時における沈降物に含まれる有機態の炭素量および窒素量は夜光虫赤潮時と同様に非ブルーム時より高く，サルパ・ブルーム時の沈降物中の C/N（モル比）は，非サルパ・ブルーム時よりサルパの体と糞に近い値であった（Table 1）．サルパは，他の動物プランクトンより高いろ水能力を有し（ALLDREDGE and MADIN, 1982），植物プランクトン，微小動物プランクトンおよび懸濁態粒子を非選択的に摂食する（SILVER, 1975; HUNTLEY *et al.*, 1989; NISHIKAWA *et al.*, 1995; 西川, 2001, 2003; VARGAS and MADIN, 2004）．さらにサルパによる直接摂食のみならず，他の植食性動物プランクトンは，サルパと餌をめぐる競合に負けた結果間接的に排除される場合があることが指摘されている（NISHIKAWA *et al.*, 1995; 西川, 2001; PERISSINOTTO and PAKHOMOV, 1998）．そのためサルパ・ブルーム形成海域おいて，他の生物量や懸濁態粒子の著しい減少がみられ（BATHMANN, 1988; ZELDIS *et al.*, 1995; 西川, 2001; GIESECKE *et al.*, 2014），ほぼサルパの独占状態になる（西川, 2001; GIESECKE *et al.*, 2014）．従って，下波湾のサルパ・ブルーム時に底層に輸送された沈降物中の有機物は主にサルパ由来のものである可能性を示唆する．これまでも，サルパ由来有機物の底層への輸送に関する報告は，多くの海域においてなされている（ISEKI, 1981; MADIN, 1982; MORRIS *et al.*, 1988）．MORRIS *et al.* (1988) は，地中海ヴィルフランシュ湾におけるトガリサルパ・ブルーム期の有機物フラックスは，非ブルーム期の数十倍になることもあることを報告している．下波湾の透明度がサルパ・ブルームの後期には上昇していること（4月26日: 8.5m から 5月6日：17.5 m）から，表層水中の植物プランクトン等有機物を含む懸濁物は，サルパにより大量にろ過され糞として凝集後体外へ放出され，糞はサルパが放出する粘性を有する網に付着する

Table 1 Organic carbon and nitrogen of settling matter, and fecal pellets and body of salp (*Salpa fusiformis*)

Trap experiment period and salp-derived matter	Settling matter		C/N
	(mgC g⁻¹)	(mgN g⁻¹)	(mol mol⁻¹)
Salp bloom (6-8 May)	42.8	8.58	5.82
Noctiluca red tide (11-13 May)	48.4	8.10	6.97
Non-bloom (17-19 May)	12.1	1.64	8.63
Non-bloom (24-26 May)	5.50	0.82	7.86
Fecal pellets of salps	115	24.4	5.49
Salp body	35.5	8.67	4.78

ことで一時的にヌタとして浮遊するものの，付着していく懸濁物の重みにより最終的には底層へ素早く沈降していくものと考えられる．調査海域の底質は砂状で有機物は少ないことから，サルパによって表層からもたらされる有機物は底生生物の餌として大きく寄与しているものと考えられ，沈降したサルパ由来有機物が底層の生態系にどのように利用されているのか等について詳細な調査が必要になる．

謝　辞

参考文献

ALLDREDGE, A. L. and L. P. MADIN (1982): Pelagic tunicates: unique herbivores in the marine plankton. Bioscience, **32**, 655-663.

BATHMANN, U. V. (1988): Mass occurrence of *Salpa fusiformis* in the spring of 1984 off Ireland: implications for sedimentation processes. Mar. Biol., **97**, 127-135.

BONE, Q., C. CARRE and K. P. RYAN (2000): The endostyle and feeding filter in salps (Tunicata). J. Mar. Biol. Ass. U. K., **80**, 523-534.

BRACONNOT, J. C. (1971): Contribution à l'étude biologique et écologique des Tuniciers pélagiques Salpides et Doliolides I. Hydrologie et écologie des Salpides. Vie Milieu, **22**, 257-286.

CHAE, J., H. W. CHOI, W. J. LEE, D. KIM and J. H. LEE (2008): Distribution of a pelagic tunicate, *Salpa fusiformis* in warm surface current of the eastern Korean waters and its impingement on cooling water intakes of Uljin nuclear power plant. J. Environ. Biol., **29**, 585-590.

FRANCO, P., H. CHEN and G. LIU (2014): Distribution and abundance of pelagic tunicates in the North Yellow Sea. J. Ocean Univ. China, **13**, 782-790.

藤井誠二 (2007)：発電所の取水口を詰まらせる新手の迷惑生物．海生研ニュース, **96**, 11.

GIESECKE, R., A. CLEMENT, J. GARCÉS -VARGAS, J. I. MARDONES, H. E. GONZÁLEZ, L. CAPUTO and L. CASTRO (2014): Massive salp outbreaks in the inner sea of Chiloé Island (Southern Chile): possible causes and ecological consequences. Lat. Am. J. Aquat. Res., **42**, 604-621.

HUNTLEY, M. E., P. F. SYKES and V. MARIN (1989): Biometry and trophodynamics of *Salpa thompsoni* Foxton (Tunicata; Thaliacea) near the Antarctic Peninsula in austral summer, 1983-1984. Polar Biol., **10**, 59-70.

IGUCHI, N. and T. IKEDA (2004): Metabolism and elemental composition of aggregate and solitary forms of *Salpa thompsoni* (Tunicata: Thaliacea) in waters off the Antarctic Peninsula during austral summer 1999. J. Plankton Res., **26**, 1025-1037.

飯田直樹 (2009)：刺網に付着していた泥状の物質の正体について．富水研だより, **2**, 10-11.

ISEKI, K. (1981): Particulate organic matter transport

to the deep sea by salp fecal pellets. Mar. Ecol. Prog. Ser., **5**, 55-60.

兼田淳史・小泉喜嗣・高橋大介・福森香代子・郭新宇・武岡英隆 （2010）：2007 年宇和海下波湾における有害渦鞭毛藻 *Karenia mikimotoi* 赤潮の底入り潮の発生による消滅．水産海洋研究, **74**, 167-175.

小泉喜嗣 （2002）：豊後水道東岸域における急潮と植物プランクトンの増殖機構に関する研究．愛媛県水産試験場研究報告, **10**, 1-91.

黒田一紀・森本晴之・井口直樹 （2000）：2000 年の日本海におけるサルパ類とクラゲ類の大量出現．水産海洋研究, **64**, 311-315.

LICANDRO, P., F. IBAÑEZ and M. ETIENNE （2006）: Long-term fluctuations （1974-1999） of the salps *Thalia democratica* and *Salpa fusiformis* in the northwestern Mediterranean Sea: Relationships with hydroclimatic variability. Limnol. Oceanogr., **51**, 1832-1848

LIU, Y., S. SUN and G. ZHANG （2012）: Seasonal variation in abundance, diel vertical migration and body size of pelagic tunicate *Salpa fusiformis* in the Southern Yellow Sea. Chin. J. Oceanol. Limnol., **30**, 92-104.

MADIN, L. P. （1982）: Production, composition and sedimentation of salp fecal pellets in oceanic waters. Mar. Biol., **67**, 39-45.

三島康史・門谷茂・岡市友利 （1990）：巨視的浮遊性大型粒子（NUTA）：採取装置の開発と懸濁粒子・沈降粒子との関係．La mer, **28**, 123-130.

MONTANI, S., K. TADA and T. OKAICHI （1988）: Purine and pyrimidine base in marine particles in the Seto Inland Sea, Japan. Mar. Chem., **25**, 359-371.

森実庸男 （1995）：サルパで養殖ハマチが死んだ話．愛媛水試だより, **9**, 12-14.

MORRIS, R. J., Q. BONE, R. HEAD, J. C. BRACONNOT and P. NIVAL （1988）: Role of salps in the flux of organic matter to the bottom of the Ligurian Sea. Mar. Biol., **97**, 237-241.

NISHIKAWA, J., M. NAGANOBU, T. ICHII, H. ISHII, M. TERAZAKI and K. KAWAGUCHI （1995）: Distribution of salps near the South Shetland Islands during austral summer, 1990-1991 with special reference to krill distribution. Polar Biol.,**15**, 31-39.

西川淳 （2001）：サルパ類研究のどこが面白いか？月刊海洋／号外, **27**, 207-215.

NISHIKAWA, J. and A. TSUDA （2001）: Diel vertical migration of the tunicate *Salpa thompsoni* in the Southern Ocean during summer. Polar Biol., **24**, 299-302.

西川淳 （2003）：海産ゼラチン質プランクトン，サルパ類をめぐる捕食と被食．日本プランクトン学会報, **50**, 98-103.

西村三郎 （1958）：中部日本海産マサバの攝餌に関する一知見―トガリサルパの攝取について―．日水研年報, **4**, 105-112.

ONO, A., T. ISHIMARU and Y. TANAKA （2010）: Distribution and population structure of salps off Adelie Land in the Southern Ocean during austral summer, 2003 and 2005. La mer, **48**, 55-70.

PAGÈS, F., H. E. GONZÁLEZ, M. RAMÓN, M. SOBARZO and J.-M. GILI （2001）: Gelatinous zooplankton assemblages associated with water masses in the Humboldt Current System, and potential predatory impact by *Bassia bassensis* （Siphonophora: Calycophorae）. Mar. Ecol. Prog. Ser., **210**, 13-24.

PERISSINOTTO, R. and E. A. PAKHOMOV （1998）: The trophic role of the tunicate *Salpa thompsoni* in the Antarctic marine ecosystem. J. Mar. Sys., **17**, 361-374.

SILVER, M. W. （1975）: The habitat of *Salpa fusiformis* in the California Current as defined by indicator assemblages. Limnol. Oceanogr., **20**, 230-237.

多田邦尚・門谷茂・VEERAPORN SUKSOMJIT・広瀬敏一・一見和彦 （2009）：ハマチ *Seriola quinqueradiata* 養殖場における沈降粒子束．日水誌, **75**, 383-389.

武岡英隆・秋山秀樹・菊池隆展 （1992）：豊後水道の急潮．沿岸海洋研究ノート, **30**, 16-26.

VARGAS, C. A. and L. P. MADIN （2004）: Zooplankton feeding ecology: clearance and ingestion rates of the salps *Thalia democratica*, *Cyclosalpa affinis* and *Salpa cylindrical* on naturally occurring particles in the Mid-Atlantic Bight. J. Plankton Res., **26**, 827-833.

山下亜純・井関和夫・樽谷賢治・小泉喜嗣 （2011）：宇和海下波湾における基礎生産速度の季節変動．水産海洋研究, **75**, 9-18.

ZELDIS, J. R., C. S. DAVIS, M. R. JAMES, S. L. BALLARA, W. E. BOOTH and F. H. CHANG （1995）: Salp grazing: effects on phytoplankton abundance, vertical

distribution and taxonomic composition in a coastal habitat. Mar. Ecol. Prog. Ser., **126**, 267-283.

A new simplified method for the measurement of water-leaving radiance

Motoaki Kishino[1)2)]* and Ken Furuya[1)]

Abstract: A new simplified method to measure water-leaving radiance was developed by combined use of a miniature spectrophotometer, a collimator, and a narrow pipe to block reflected sunlight from the sea surface. The instrument was handy, light-weighted and least expensive compared with those available for commercial use. The water-leaving radiance was determined by using the above-mentioned setup in the East China Sea, the Seto Inland Sea, and Shonai-ko of Lake Hamana. These areas covered a wide range of water mass types from clear to turbid water, and the new method was successfully implemented in all the areas. Signal to noise ratios of remote sensing reflectance R_{rs} measured by the instrument were satisfactorily small by taking running mean of 7 data readings over about 1.3 nm and by sampling of 1 nm interval. However, noises were not negligible in a low R_{rs} range below 0.001 sr^{-1} which occurred in the longer wavelength range than 650 nm. The estimated errors due to self-shading were satisfactorily small ($< 5\%$) in the wavelength range from 400 to 590 nm.

Keywords: *water-leaving radiance, ocean-color remote sensing, spectrophotometer, USB4000*

1. Introduction

Water-leaving radiance, which is the upwelling radiance emitted from the sea to the air, is one of the most important parameters for ocean-color remote sensing. Water-leaving radiance is determined from the total radiance measured by satellite ocean-color sensors with the implementation of atmospheric correction (Gordon and Clark, 1980; Fukushima *et al.*, 1998). However,

1) Department of Aquatic Bioscience, The University of Tokyo, Yayoi 1-1-1, Bunkyo, Tokyo 113-8657, Japan
2) Present address: Nishibori 5-2-10-115, Sakuraku, Saitama 338-0832, Japan
＊Corresponding author: Motoaki Kishino
e-mail: mkishino@f8.dion.ne.jp

the obtained water-leaving radiance is dependent on both solar altitude and the conditions of the air parameters used for the correction. Therefore, it is essential to validate the atmospheric corrections and in-water algorithms in order to determine the water-leaving radiance in situ. In ocean-color remote sensing, remote sensing reflectance, which is the water-leaving radiance divided by the incident solar irradiance just above the sea surface, is used to retrieve properties of seawater, including chlorophyll *a* concentration, suspended mater, and dissolved organic matter (Gordon and Morel, 1983; Kishino *et al.*, 1998; O'Reilly *et al.*, 1998). Thus, water-leaving radiance is a key parameter in ocean-color remote sensing and is used not only for validations, but also for the development of new in-water algorithms. Water-

leaving radiance also allows for the vicarious calibration of the satellite ocean-color sensors (MᴄCʟᴀɪɴ *et al.*, 2000).

Water-leaving radiance is usually measured by a spectrophotometer mounted on a tower top or on the upper deck of a research vessel. The present communication describes a new simplified method for the in situ measurement of the water-leaving radiance by using convenient and less expensive instrumentation when compared with commercially available instruments.

2. Issues associated with conventional methods

Water-leaving radiance is measured from the upwelling radiance at, or near, the sea surface by the use of an in-water spectrophotometer (e.g., PRR-800, SuBOPS) (Kɪsʜɪɴᴏ *et al.*, 1997; Mᴏʀʀᴏw *et al.*, 2010), from the calculations on a handheld instrument (e. g., SIMBAD), or from a photometer system (e. g., RAMSES, SeaPRISM) mounted on the upper deck or tower top of a research vessel (Hᴏᴋᴋᴇʀ *et al.*, 2000; Isʜɪᴢᴀᴋᴀ *et al.* personal communications). The direct measurement of water-leaving radiance needs to avoid the sea surface reflectance (Tᴀɴᴀᴋᴀ *et al.*, 2006; Lᴇᴇ *et al.*, 2013).

An underwater spectrophotometer used for the estimation of water-leaving radiance consists of an onboard spectral irradiance meter, an underwater unit fitted with a downwelling irradiance meter and an upwelling radiance meter, and an interface unit that has a battery power source. The attenuation coefficient of the upwelling radiance, K_u, is calculated from an upwelling radiance profile near the sea surface, L_u (z, λ):

$$K_u(\lambda) = \frac{1}{(z_1 - z_0)} \ln \frac{L_u(z_0, \lambda)}{L_u(z_1, \lambda)}.$$

Then, the upwelling radiance just below the sea surface, L_u (0^-, λ), is extrapolated:

$$L_u(0^-, \lambda) = L_u(z_0, \lambda) \exp[z_0, \lambda] \exp[z_0, K_u(\lambda)].$$

The water-leaving radiance, L_w (λ), is calculated from L_u (0^-, λ), which, according to Aᴜsᴛɪɴ (1974), is:

$$L_w(\lambda) = \frac{1 - \rho(\lambda)}{n(\lambda)^2} L_u(0^-, \lambda).$$

where $\rho(\lambda)$ is the Fresnel surface reflectance and n (λ) is the refractive index of seawater. The remote sensing reflectance, R_{rs} (λ), is obtained from L_w (λ) and the spectral irradiance of the incident sea surface, E_{ds} (λ):

$$R_{rs}(\lambda) = \frac{L_w(\lambda)}{E_{ds}(\lambda)} = \frac{1 - \rho(\lambda)}{n(\lambda)^2} \frac{L_u(0^-, \lambda)}{E_{ds}(\lambda)}..$$

The normalized water-leaving radiance, L_{nw} (λ), can be obtained from the remote sensing reflectance and extraterrestrial solar irradiance, F_o (λ):

$$L_{nw}(\lambda) = F_o(\lambda) \times R_{rs}(\lambda).$$

Errors in the estimation of water-leaving radiance are considered to originate from the self-shading caused by the size of the photometer (Aᴀs, 1969; Tᴀɴᴀᴋᴀ *et al.*, 2006) and the variations in measured radiance and the depth caused by sea surface wave motion. However, the data measured by an underwater photometer are used not only to estimate water-leaving radiance, but also to determine the spectral distribution of underwater light in optical studies of light field and phytoplankton photosynthesis.

In general practice, a photometer system mounted on the upper deck or a tower top of a research vessel is composed of an irradiance meter and two radiance meters (Fig. 1). The irradiance meter measures the incident irradiance at the sea surface. The radiance meter is directed at the sea surface with a tangential angle
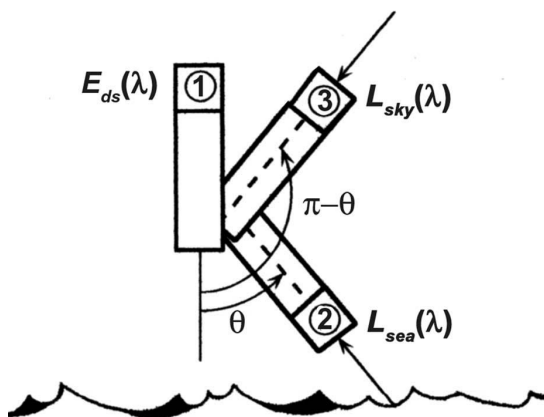
Fig. 1 A schematic of the instruments on the top of the tower. For details, see text.

  1 : Irradiance meter for incident irradiance at the sea surface

  2 : Sea-viewing radiance meter for total radiance (above the surface)

  3 : Sky-viewing radiance meter for indirect radiance

(θ) of 30° to 45° from the vertical axis and measures the total radiance, including the water-leaving radiance and the refracted sky radiance from the sea surface. The other radiance meter is directed towards the sky with an angle of 30° to 45° from the zenith axis ($\pi-\theta$) and measures the sky radiance.

The two radiances and the irradiance are calculated by using remote sensing reflectance (HOOKER *et al.*, 2003):

$$R_{rs}(\lambda)=[L_{sea}(\lambda)-rL_{sky}(\lambda)]/E_{ds}(\lambda),. ,$$

where $L_{sea}(\lambda)$ is the total radiance (including water-leaving radiance and refracted sky radiance on the sea surface), r is the sea surface reflectance, $L_{sky}(\lambda)$ is the sky radiance, and $E_{ds}(\lambda)$ is the incident irradiance of the sea surface.

Ishizaka and his group attempted to use a photometer system mounted on the upper deck of the express liners between Fukuoka and Pusan (ISHIZAKA, personal communication) to calculate the chlorophyll concentration along the cruise tracks. Their attempt resulted in limited success, mainly because the reflected sky radiance fluctuated in accordance with the roughness of the sea surface, the ship's shadow, and white bubbles. Thus, it is difficult to obtain a stable measurement of the radiance. If water-leaving radiance has a bi-directional function, the normalized water-leaving radiance can have large errors.

A method for the direct measurement of water-leaving radiance was proposed by TANAKA *et al.* (2006), who used the RAMSES-ARC (TriOS GmbH) as a radiance sensor. They measured the water-leaving radiance with an underwater spectral upwelling radiometer, PRR-800, in Katagami Bay, Nagasaki, on the west side of Kyusyu, Japan. However, a dome cover used by TANAKA *et al.* (2006) resulted in large errors due to self-shading because the dome was too large, measuring 15 cm in diameter (GORDON and DING, 1992).

3. Direct measurement of water-leaving radiance

For the direct measurement of the water-leaving radiance, we present a new simplified instrument that is composed of a miniature spectrophotometer (USB-4000, Ocean Optics) connected with a collimator placed at the top end of an opaque vinyl chloride pipe (Fig. 2). A major advantage of the USB-4000 is its portability with a reasonable price, and wavelength resolution. A total cost of the proposed system including a PC is less than one third of that of RAMSES (TriOS) of a similar sensing configuration to the proposed one. RAMSES is installed in a pressure-resistant container which enables its use down to 300 m depth. But, we do not need such consideration to hydro-pressure in our purpose to measure at the
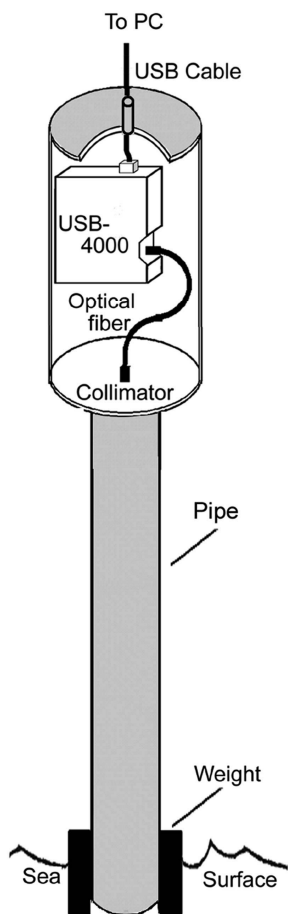
Fig. 2 Configuration of a new simplified instrument

surface. Furthermore, the USB-4000 provides the output of a finer wavelength resolution than that of RAMSES, as exemplified by an observation that the former can detect sharp emission lines of fluorescence tubes, but the latter gives only their broad peaks.

The detector of the USB-4000 has a CCD array, which has 3648 elements. The wavelength range is between 400 nm and 750 nm. The overall wavelength resolution is approximately 1.33 nm with 25 μ m of the entrance aperture of spectrometer. The pipe is 5 cm in diameter and 50 cm long, whose inside is painted black to prevent reflection. The field of view of the radiance meter

is limited to 5° 45′ by the diameter of the pipe. The signals from the spectrophotometer are sent to a PC via a USB cable. The other end of the pipe is fitted with a 2-kg weight to keep the pipe in a vertical position and soaked in seawater in order to measure the water-leaving radiance without interference from the reflected sky radiance. In the actual measurements, the instrument was hanged by a thin rope to keep the instrument stably at the vertical direction with the other end of a pipe dipped into the water within 10 cm.

In general practice, the incident irradiance (E_{ds}) of the sea surface is obtained from radiance measured by a standard white diffuser, and the radiance reflected from the standard diffuser tends to be higher than the water-leaving radiance. However, since the remote sensing reflectance is generally in the range of 0.002 sr^{-1} or 0.003 sr^{-1}, occasionally exceeding 0.01 sr^{-1} between 500 nm and 555 nm, the instrumental sensitivity has to be raised for measurement of the water-leaving radiance. Here, we propose the use of a gray reflectance plate as a substandard. This enables to maintain the same instrumental sensitivity for measurement of both incident and water-leaving radiance. This procedure facilitates measurements by easy comparison of both measurements, and by eliminating switching the instrumental sensitivity. The gray plate was made of a homogeneous mixture of plaster and black India ink. The reflectance of the plate followed the cosine law and approximately 10% of reflectance intensity compared with a commonly used white standard was most convenient. In the following measurements, we used a gray plate of 11% reflectance. The incident irradiance at the sea surface, E_{ds} (λ), is obtained as follows:

$$E_{ds}(\lambda) = \pi L_G(\lambda)/G_r(\lambda).$$

Then, the remote sensing reflectance, R_{rs} (λ), is

$$R_{rs}(\lambda) = \frac{L_w(\lambda)}{\pi L_G(\lambda)/G_r(\lambda)} = \frac{L_w(\lambda)}{E_{ds}(\lambda)},$$

where $L_G(\lambda)$ and $G_r(\lambda)$ are the radiance and reflectance of the gray plate, respectively.

While the proposed instrument does not have an optical shutter, the dark current can be monitored by covering with a cap at the end of measuring pipe. Next, after removing the cap, water-leaving radiance, $L_w(\lambda)$, is measured. Then the dark value is re-confirmed with the cap again. The influence of temperature dependence on dark current is eliminated in this way. In a similar manner, the incident irradiance at the sea surface, $E_{ds}(\lambda)$, is measured using the gray diffuser. The time required is within 5 minute.

4. Measurement

The new method was verified by in situ tests in the East China Sea, the Seto Inland Sea, and Shonai-ko of Lake Hamana. The test in the East China Sea was conducted on September 5–13, 2007 during the RV Tansei Maru cruise (KT–07–22) within Kuroshio, where the water was very clear and blue in color. The Seto Inland Sea was surveyed on board the RV Nauplius on July 19 and August 24, 2007, when dense blooms of diatoms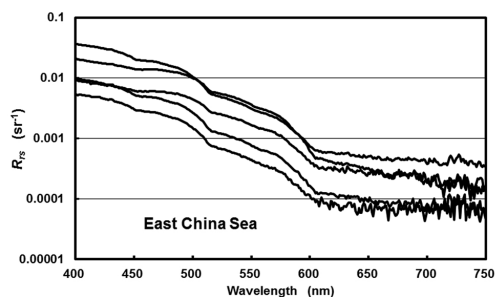 occurred off Harimanada with yellow-ish green color at the surface. Shonai-ko of Lake Hamana was visited on July 9 and 17, 2008, when mixed red tides of diatoms and dinoflagellates occurred, which caused the water to take on the color of soy sauce. R_{rs} was obtained by running mean of 7 consecutive data readings over about 1.3 nm, and by sampling of 1 nm interval based on preliminary examinations to reduce influences of noise.

Concentrations of chlorophyll a were very low, ranging between 0.03 and 0.15 mg m^{-3}, in the East China Sea, and typical reflectance in blue water was observed. Remote sensing reflectance in the East China Sea was high at short wavelengths and decreased toward longer wavelengths to reach almost zero at a wavelength of 600 nm (Fig. 3).

The concentrations of chlorophyll a varied considerably, ranging from 0.35 to 14.24 mg m^{-3}, in the Seto Inland Sea. Remote sensing reflectance showed peaks at wavelengths around 580 nm and at 685 nm (Fig. 4). The latter maximum was the result of chlorophyll fluorescence (KISHINO et al., 1984).

The remote sensing reflectance at Shonai-ko of Lake Hamana was high, ranging between 500 and 650 nm, and exhibited a maximum at a wavelength of 700 nm (Fig. 5). These high values resulted from a combination of scattering and fluorescence and appeared to shift towards longer wavelengths (KISHINO et al., 1986). Small

Fig. 3 Remote sensing reflectance R_{rs} in the East China Sea measured between 10:00 and 15:00 on September 5–13, 2007 during the RV Tansei Maru cruise (KT–07–22).
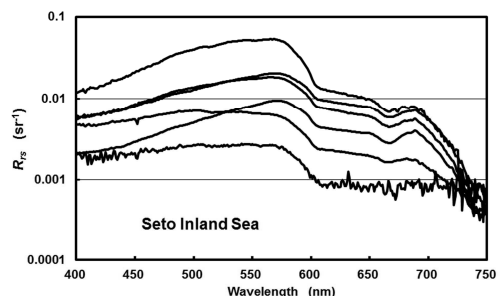

Fig. 4 Remote sensing reflectance R_{rs} in the Seto Inland Sea measured on July 19, 2007.

maximums were found at wavelengths of 560 to 600 nm and 645 nm. These maximums corresponded to the minimum of dinoflagellates absorption. The concentration of chlorophyll a ranged from 13.75 at the mouth of the lake to 77. 98 mg m^{-3} at its innermost part.

R_{rs} measured by the new instrument and PRR-800 was compared by simultaneous measurements of both instruments at 6 stations during the KT07-22 cruise. R_{rs} were calculated using USB-4000 fitted with band-pass filters with band width of $\pm$ 10 nm, and from E_{ds} and L_u obtained by using PRR-800. No significant variation in observation was noted among stations, and an example at a station was shown in Fig. 6. Both instrument yielded similar R_{rs} values in the range of 380 -- 595 nm with a considerable discrepancy of USB 4000 from PRR-800 beyond 625 nm, probably due to electrical noise of USB-4000. Correlation coefficients at 6 stations varied between 0.949 and 0.999 with a mean of 0.987 $\pm$ 0. 0018. between values obtained by both instruments. Thus, R_{rs} obtained by both instruments can be regarded as identical below 595 nm.

Signal to noise ratio of the new instrument was examined. Signal-to-noise ratio of USB-4000 was 300: 1 at full signal according to instrumental specifications. The integration time was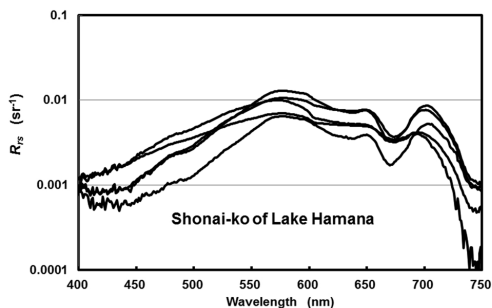 set at 100 msec at the high solar altitude. During a measurement conducted in clear ocean off Okinawa Islands in the East China Sea at 10:36 local time on 7 September, 2007, the solar radiance reflected by gray plate, L_G was 5000 at the wavelength of 400 nm, increased to 42000 at 535 nm, and decreased to 15800 at 750 nm. This spectral distribution was almost identical to the spectral sensitivity of USB-4000. Noises fluctuated between 200 and 400 in the wavelength range from 400 to 750 nm. Then, signal to noise ratio was calculated to range between 12.5:1 and 107.5:1. The radiance from the sea surface, L_w was 2550 at 400 nm, increasing to 5700 at 490 nm, decreasing to 400 at 600 nm, and 150 at 750 nm with noises ranging from 100 to 200 in the whole wavelength. Then, signal to noise ratio in the range from 400 to 600 nm varied from 2:1 to 28.5:1, and 0.75:1 to 2:1 in the range between 600 and 700 nm.

A similar analysis was made for turbid water at Shonai-ko of Lake Hamana at local time of 13:50 15 July, 2008, the solar radiance reflected by gray plate, L_G, was 3000 at the wavelength of 400 nm, was increasing to 32000 at 535 nm, and decreasing to 11000 at 750 nm. The noises were between 200 and 400 at wavelength from 400 to 750nm.

Fig. 5   Remote sensing reflectance R_{rs} at Shonai-ko of Lake Hamana measured on July 15, 2008.
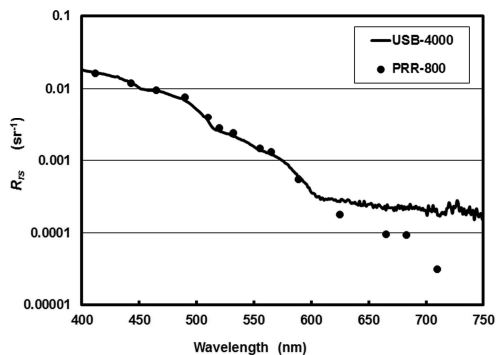

Fig. 6   Comparison of remote sensing reflectance R_{rs} measured by PRR-800 and USB-4000 in the East China Sea. Circles and a solid line denote values obtained by PRR-800 and USB-4000, respectively.

Then, signal to noise ratio ranged between 7.5:1 and 80:1. The radiance from the sea surface, L_w was 200 at 400 nm, increased to 1200 at 500 nm, reached its maximum of 6500 at 580 nm, and decreased to 400 at 750 nm. Another secondary maximum of 2450 due to chlorophyll a fluorescence appeared at around 700 nm. The noises ranged between 100 and 200 at whole wavelength. Then, signal to noise ratio varied from 1:1 to 32.5:1 in the wavelength range from 400 to 600 nm, and from 2:1 to 15.1:1 between 600 and 750 nm except the wavelength range between 675 and 710 nm, where signal to noise ratio was large due to the chlorophyll a fluorescence.

These noise levels were reduced much to one third or fourth by taking a running mean of 7 data readings and by sampling at interval 1 nm. However, noises were not negligible even with this treatment in low R_{rs} range below 0.001 sr^{-1}, which occurred in the longer wavelength range than 650 nm (Figs. 3, 4 and 5).

5. Discussion

The advantages of the new method are as follows: (1) it allows direct measurement of water-leaving radiance without the interference of reflected radiance at the sea surface; (2) it is handy for use on small boats; (3) there is no need for absolute calibration; and (4) it is inexpensive to make. A possible disadvantage is errors caused by the uncertainty of the depth of the bottom end of the pipe. The error becomes large with increasing depth of the bottom end and turbidity of seawater. The lack of need for absolute calibration means that the calibration errors would be less than 5% (MUELLER and AUSTIN, 1992). Other errors are caused by the ship's effects and self-shading. As is common in optical measurements, the new method is under the influence of the ship's shade (GORDON, 1985; SARUYA et $al.$, 1997; Leathers et $al.$, 2004).

According to the results of a Monte Carlo simulation and its field validation by SARUYA et $al.$ (1997), the error in upward irradiance is much smaller than that for downward irradiance, but it is not negligibly small. Therefore, the use of a boom in order to avoid the shade is recommended.

Let us consider errors associated with self-shading. GORDON and DING (1992) estimated the diameter (D_{max}) of an optical instrument that produced an error of 5% of R_s by the Monte-Carlo technique, and they showed an error associated with self-shading, ε of an instrument whose diameter is D as:

$$\varepsilon = 1\text{-} (0.95)\ D/D_{max},$$

Using this relationship and Figure 11 of GORDON and DING (1992), errors due to self-shading of the new instrument was estimated to be 1% or 2% between 350 nm and 590 nm, and lower than 5% from 600 nm to 650 nm when chlorophyll a concentration was 1 mg m^{-3}. In the longer wavelength range, the error increased to about 9% at 700 nm and sharply to about 30% at 740 nm. With high chlorophyll a concentration of 10 mg m^{-3}, the error increased to 2% or 3% between 350 nm and 580 nm, and below 5% between 590 and 640 nm. In the case of the PRR-800, the diameter of the photometer is 10.2 cm, and the error for water with chlorophyll a concentration of 1 mg m^{-3} would be below 5% between 350 nm and 570 nm. In case of 10 mg m^{-3} chlorophyll a, the errors would be lower than 5% at around 540 nm and below 7% at wavelength shorter than 590 nm. At longer wavelength the error increased sharply, for example, 17% at 700 nm, and over 50% at 740 nm. Based on these consideration, errors due to self-shading of the new instrument is half as that of PRR-800.

Let us consider a case where the water-leaving

radiance is estimated by the upward spectral radiance measured at 1 m depth by using an underwater spectral irradiance meter. If the depth has an error of ± 0.1 m, then the error would be under 1% when k_u is 0.05 m^{-1} for very clear ocean water, ± 5% when k_u is 0.5 m^{-1}, and about ± 10% when k_u is 1 m^{-1} in turbid coastal areas. It is believed that the water-leaving radiance can be estimated from 2 m depth. The error would be ± 1%, ± 10%, and ± 20% for k_u values of 0.05 m^{-1}, 0.5 m^{-1}, and 1 m^{-1}, respectively. The error would become larger for larger values of k_u and greater measured depths. The spectral attenuation coefficient of upward radiance, k_u (λ), changes with wavelength, especially at large wavelengths. Thus, the error varies considerably with both depth and wavelength.

The reflected sky radiance by the sea surface is added to the water-leaving radiance in the case of tower or shipboard measurements. Water-leaving radiance can be obtained by the revision of the total sea radiance using the reflectance of the sea surface. The reflectance of the sea surface depends on the incident angle and surface conditions. The reflectance of a mirror-like sea surface follows Fresnel's law. The reflectance under an incident angle of 40° is about 2%, whereas reflectance values at incident angles greater than 40° can be up to 100% at 90°. In contrast, while the reflectance from wavy sea surface is a little larger than that of a flat surface at small incident angles, the reflectance at large incident angles is smaller than that of a flat surface (BURT, 1954; COX and MUNK, 1956; HISHIDA and KISHINO, 1965). Thus, the reflected radiance varies considerably in response to wave action. However, the reflectance is often regarded as a constant in the measurement of the water-leaving radiance in the case of the tower or shipboard is often used as a constant. For example, HOKKER *et al.* (2003) used 2.8% for the

reflectance of the sky radiance at tower measurements. In addition, other factors than sea conditions must also be considered in the measurement of reflectance. The new simplified instrumentation is expected to facilitate in situ measurement of water-leaving radiance.

In conclusion, the new proposed pipe method for the direct measurement of water-leaving radiance is convenient and applicable in the field from the clear open ocean to turbid coastal or lake water environments. Moreover, the errors obtained are smaller than those obtained with previous methods.

Acknowledgements

References

AAS, E. (1969): On submarine irradiance measurements. Rep. Dept. Phys. Oceanogr. **6**, Univ. Copenhagen, 51pp.

AUSTIN, R. W. (1974): The remote sensing of spectral radiance from below the ocean surface. *In* Optical Aspects of Oceanography. Jerlov, N. G. and E. S. Nielsen (eds.), Academic Press, London, p. 317–344.

BURT, W. V. (1954): Albedo over wind-roughened water. J. Meteorol., **15**, 76–80.

COX, C. and W. MUNK (1956): Slopes of the sea surface deduced from photographs of sun glitter. Bull. Scrips Inst. Oceanogr. Univ. Calif., **6**, 401–488.

FUKUSHIMA, H., A. HIGURASHI, Y. MITOMI, N. NAKAJIMA, T. NOGUCHI, T. TANAKA and M. MITOMI (1998): Correction of atmospheric effects on ADEOS/OCTS ocean color data: Algorithm description and evaluation of its performance. J. Oceanogr., **54**,

417–430.

GORDON, H. R. (1985): Ship perturbation of irradiance measurements at sea: Monte Carlo simulations. Appl Opt, **24**, 4172–4182.

GORDON, H. R., and D. K. CLARK (1980): Atmospheric effects in the remote sensing of phytoplankton pigments. Boundary Layer Meteol., **18**, 299–313.

GORDON, H. R., and K. DING (1982): Self-shading of in-water optical instruments. Limnol. Oceanogr., **37**, 491–500.

GORDON. H. R., and A. MOREL (1983): Remote assessment of ocean color for interpretation of satellite visible imagery. *In* A Review, Lecture Notes on Coastal and Estuarine Studies. Barber, R. T., N. K. Mooers, M. J. Bowman and B. Zeitzschel (eds.), Springer-Verlag, New York, 114pp.

HISHIDA, K, and M. KISHINO (1965): On the albedo of radiation of the sea surface. J. Oceanogr. Soc. Japan., **21**, 148–153.

HOOKER, S. B, G. ZIBORDI, S. W. BAILEY and C. M. PIETRAS (2000): The SeaWiFS photometer revision for incident surface measurement (SeaPRISM) field commissioning. *In* SeaWiFS Postlaunch Tech. Rep. Ser. Hooker, S. B. and E. R. Firestone (eds.), NASA Tech. Memo. 2000–206892, Vol. 13. NASA Goddard Space Flight Center, Greenbelt, Maryland, 24pp.

HOOKER, S. B., G. ZIBORDI, J-F. BERTHON, D. D'ALIMONTE, D. van der Linde and J. W. Brown (2003): Tower-Perturbation Measurements in Above-Water Radiometry. *In* SeaWiFS Postlaunch Tech. Rep. Ser. Hooker, S. B. and E. R. FIRESTONE (eds.), NASA Tech. Memo. 2003–206892, Vol. 23. NASA Goddard Space Flight Center, Greenbelt, Maryland, 35pp.

KISHINO M,. T. ISHIMARU and F. FURUYA, T. OISHI and K. KAWASAKI (1998): In-water algorithms for ADEOS/OCTS. J. Oceanogr., **54**, 431–436.

KISHINO M., J. ISHIZAKA, S. SAITOH, Y. SENGA and M. UTASHIMA (1997): Verification plan of ocean color and temperature scanner atmospheric correction and phytoplankton pigment by moored optical buoy system. J. Geophys. Res., **102**, 17197–17207.

KISHINO, M, S. SUGIHARA and N. OKAMI (1984): Influence of fluorescence of chlorophyll *a* on underwater upward irradiance spectrum. La mer, **22**, 224–232.

KISHINO M,. S. SUGIHARA and N. OKAMI (1986): Theoretical analysis of the in situ fluorescence of chlorophyll *a* on the underwater spectral irradiance. La mer, **24**, 130–138.

LEATHERS, R. A., T. V. DOWNES and C. D. MOBLEY (2004): Self-shading correction for oceanographic upwelling radiometers. Opt. Express, **12**, 4709–4718.

LEE, Z. P., N. PAHLEVA, Y. H. AHN, S. GREB and D. O' DONNELL (2013): Robust approach to directly measuring water-leaving radiance in the field. Appl. Opt., **52**, 1693–1701.

MCCLAIN, C. R., E. J. AINSWORTH, R. A. BARNES R. E. EPLEE, Jr., F. S. PATT, W. D. ROBINSON, M. WANG and S. W. BAILEY (2000): SeaWiFS postlaunch calibration and validation analyses, Part 1. *In* SeaWiFS Postlaunch Tech. Rep. Ser. HOOKER, S. B. and E. R. FIRESTONE (eds.), NASA Tech. Memo. 2000–206892, Vol. 9, NASA Goddard Space Flight Center, Greenbelt, Maryland, 82pp.

MORROW, J. H., S. B. HOOKER, C. R. BOOTH, G. BERNHARD, R. N. LIND and J. W. BROWN (2010): Advances in measuring the apparent optical properties (AOPs) of Optically Complex Waters. *In* SeaWiFS Tech. Rep. Ser. NASA Tech. Memo. 2010–215856. NASA Goddard Space Flight Center, Greenbelt, Maryland, 80pp.

MUELLER, J. L. and R. W. AUSTIN (1992): Ocean Optics Protocols for SeaWiFS Validation. *In*: HOOKER, S. B. and E. R. FIRESTONE (eds.) NASA Tech. Memo. 104566, Vol. 5, NASA Goddard Space Flight Center, Greenbelt, Maryland, 43pp.

O'REILLY, K. L., S. MARITOREN, B. G. MITCHELL, D. A. SIEGEL, K. L. CARDER, S. A. GARVER, M. KAHRU and C. MC CLAIN (1998): Ocean color chlorophyll algorithms for SeaWiFS. J. Geophys. Res., **103**, 24937–24953.

SARUYA, Y., T. OISHI, M. KISHINO, Y. JODAI, K. KADOKURA and A. TANAKA (1997): Influence ship shadow on underwater irradiance fields. *In*: Ocean Optics XIII. ACKLESON, S. G. and R. J. FROUIN (eds.) Proce. SPIE 2963, p760–765.

TANAKA, A., H. SASAKI and J. ISHIZAKA (2006): Alternative measuring method for water-leaving

radiance using a radiance sensor with a domed cover. Opt Express. **14**, 3099–3105.

学 会 記 事

1. 第 4 回幹事会議事録
   日　時：12 月 12 日（金）10 時 00 分〜11 時 30 分
   場　所：東京海洋大学　9 号館 203 号室
   参加者：小松，今脇，森永，吉田，河野，小池，荒川，柳本，内田，奥村，本多（事務）
   議事録確認：2014 年 11 月 14 日開催の第 3 回幹事会議事録を承認
   1）　報告事項
   ①　La mer 第 52 巻第 4 号発送予定（吉田）
   ②　平成 26 年 12 月 8 日に開催された日仏関連学会協議会報告（荒川）
   ③　助成金申請状況（小松）
   　　日仏会館：次点で採択される可能性があり，1 月中に予算状況を勘案して決定される．
   　　笹川日仏財団：会長が財団へ確認する．
   ④　日仏海洋学シンポジウムについての取りまとめ記事を中野幹事が日本水産学会誌へ寄稿した旨報告された．
   ⑤　平成 26 年 11 月 17 日の平成 26 年度第 2 回水産・海洋科学研究連絡協議会，河野幹事・荒川幹事が出席した．
   ⑥　日仏海洋学会の成り立ちおよび日仏海洋学シンポジウム資料（小池）
   　　　上記資料が配布され，シンポジウムの記録とすることが説明された．
   2）　協議事項
   ①　第 16 回日仏海洋学シンポジウム（案）
   　　開催時期：2015 年 12 月上旬予定
   　　開催場所：前半は東北，最終日は日仏会館（東京）を案とする．・テーマ："The sea under human and natural impacts: challenge of oceanography to the future Earth"
   ②　委員会
   　　委員長は小松会長とした．
   　　組織委員会は幹事による委員と東北会員による委員で構成する．
   　　科学委員会：小松会長が仏日海洋学会と相談
   ③　開催趣旨
   　　資料を基に，テーマ，趣旨，セッションのア

イデアを議論した．今後，招待講演者を選ぶ．セッションのテーマとして，漁礁関連，pollution, MPA，海洋の統治関連を追加する．その他のアイデアを委員から募る．ポスターセッションも用意する．シンポジウムポスターを準備する．
   ④　会場およびプログラム（案）
   　　三陸沿岸視察（希望者）　2 日（関，小池，小松対応）
   　　仙台あるいは塩竈　1 − 2 日
   　　東京　日仏会館　1 日　（フランスからの招待者）
   　　岡山里海見学（希望者）　2 日（小松対応）
   ⑤　役割分担
   　　企画（プログラム）・広報（HP など）：柳本，内田，小松
   　　会場（懇親会会場含む）・宿泊：奥村，高見，中野
   　　予算（スポンサー／企業展示）・会計管理：森永，荒川，（本多）
   　　渉外（フランスとの窓口）：小池，小松
   　　要旨 abstract・出版：吉田，河野
   ⑥　開催費用見積りとスポンサー
   　　招待者経費，会場費などの見積をもとに，参加費について検討
   ⑦　出版
   　　学会誌 La mer の特別号査読論文として，電子出版する方向で検討
   ⑧　その他
   　　寄付依頼文の作成を荒川幹事に依頼

2. 第 5 回幹事会議事録
   日　時：2015 年 1 月 15 日（木）10 時 00 分〜12 時 00 分
   場　所：東京海洋大学　9 号館 203 号室
   参加者：小松，今脇，森永，吉田，小池，内田，柳本，關，荒川，本多（事務）
   議事録承認：2014 年 12 月 12 日開催のシンポジウム実行委員会（第 1 回）及び第 4 回幹

事会議事録を承認
1）　報告事項
2）　協議事項
第 5 回日仏海洋学会幹事会
1）　報告事項
　　　52(4) の出版と発送終了（吉田）
2）　審議事項
　①　海洋と宇宙の連携シンポジウムの共催・後援
　　　日本リモートセンシング学会からの依頼に
　　　ついて後援で対応することを決定
　②　当学会ホームページ上での論文の公開につ
　　　いて（吉田）：印刷後，即時 HP で公開するこ
　　　とを決定

3．第 6 回幹事会議事録
　　日　時：2015 年 2 月 9 日（月）10 時 30 分〜
　　場　所：東京海洋大学　9 号館 203 号室
　　参加者：小松，今脇，河野，小池，荒川，内田，
　　　　　　大越，本多（事務）
　　議事録承認：2015 年 1 月 15 日開催のシンポジウ
　　　　　　ム実行委員会（第 2 回）及び第 5 回幹事
　　　　　　会議事録を承認
1）　報告事項
　　　奥村委員が水研センターに申請した 2 名のフ
　　　ランス人研究者招請の助成金の採択（奥村）
第 6 回日仏海洋学会幹事会
1）　報告事項
　　　セカルディ先生から本学会に対して「イスラム
　　　国」による日本人人質殺害の件に哀悼の意を表
　　　するというメッセージがあったことを小池幹
　　　事より報告
2）　審議事項
　①　日仏工業技術会・在日フランス商工会議所か
　　　ら本学会あてに，JAMSTEC への見学会実
　　　施に関する協力依頼があった．今脇顧問が
　　　JAMSTEC へ取り次ぐこととした．
　②　2015 年度総会および研究発表会の日程は 6
　　　月 13 日を第 1 候補，6 日を第 2 候補とした．

4．第 7 回幹事会議事録
　　日　時：2015 年 3 月 2 日（月）10 時 30 分〜
　　場　所：東京海洋大学　9 号館 203 号室
　　参加者：小松，今脇，荒川，内田，柳本，吉田，
　　　　　　北出，小池，本多（事務）
　　議事録承認：2015 年 2 月 9 日開催のシンポジウ

ム実行委員会（第 3 回）および第 6 回幹
事会議事録の承認
第 7 回日仏海洋学会幹事会
1）　報告事項
　①　2015 年度総会および学術研究発表会の日程
　　　は，6 月 6 日（土）および 6 月 13 日（土）の
　　　会場確保ができなかったことから，6 月 27
　　　日（土）とした．
　②　2015-2016 年度学会賞選考委員の決定．（荒川）
　③　その他：La mer 第 53 巻第 1 号を準備中（吉
　　　田）

5．学会賞選考委員会半数改選が行なわれ，2015-2016
　　年度委員として，荒川久幸，石坂丞二，小松輝久，
　　多田邦尚，門谷茂が選出された．2015 年度非改選
　　委員は石丸隆，北出裕二郎，中田英昭，吉田次郎の
　　4 名．

6．退会（逝去者含む）
　　須藤英雄，有元貴文，岩重慶一，大石友彦，佐々木
　　洋，平啓介

7．所属および住所変更

氏名	新しい所属先
田　闊	浙江海洋学院水産学院
横内　一樹	独立行政法人　水産総合研究センター　増養殖研究所　資源生産部　中央水産研究所　海洋・生態系センター（併任）

8．寄贈図書
なつしま（JAMSTEC）；344〜348
農工研ニュース（農村工学研究所）；No. 94
Ocean Newsletter（海洋政策研究財団）；No. 344-349
FRAN NEWS（水産総合研究センター）；No. 41
独立行政法人　産業技術総合研究所　地質調査情報
　　センター；種子島付近表層堆積図
国立科学博物館研究報告 A 類（動物学）；第 40 巻第 4 号
年報 平成 25 年度（水産総合研究センター）
Techno-ocean News（テクノオーシャンネットワー
　　ク）；No. 55
平成 25 年度日本海ブロック資源評価担当者会議報
　　告・日本海ブロック資源研究会報告（平成 25 年度）
　　（日本海区水産研究所）
広島日仏協会報　BULLETIN　No. 196